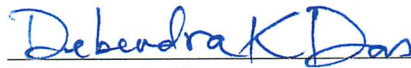


NUMERICAL STUDY OF AN EXHAUST HEAT RECOVERY SYSTEM USING  
CORRUGATED TUBES AND TWISTED TAPE INSERTS

By

Vamsi Krishna Sarma Mokkaapati

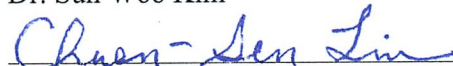
RECOMMENDED:



Dr. Debendra Das



Dr. Sun Woo Kim



Dr. Chuen-Sen Lin

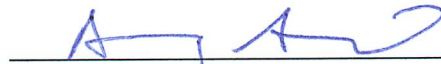
Advisory Committee Chair



Dr. Rorik Peterson, Chair

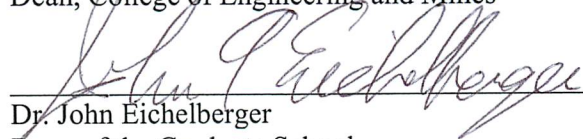
Department of Mechanical Engineering

APPROVED:



Dr. Douglas Goering

Dean, College of Engineering and Mines



Dr. John Eichelberger

Dean of the Graduate School

12/8/14

Date



NUMERICAL STUDY OF AN EXHAUST HEAT RECOVERY SYSTEM USING  
CORRUGATED TUBES AND TWISTED TAPE INSERTS

A  
THESIS

Presented to the Faculty  
of the University of Alaska Fairbanks

in Partial Fulfillment of the Requirements  
for the Degree of

MASTER OF SCIENCE

By

Vamsi Krishna Sarma Mokkaapati, B.Tech.

Fairbanks, Alaska

December 2014

## Abstract

Diesel engine generators are the major power source for small communities in cold regions. Diesel generators waste about 1/3 of their fuel energy in the form of heat through exhaust gas. The primary goal of this work is to capture part of the heat from the exhaust and improve the efficiency of the system. A gas to liquid heat transfer performance of a concentric tube heat exchanger with corrugated tubes and twisted tape inserts is investigated by considering its effects on engine performance and economics. This type of heat exchanger is expected to be inexpensive to install and effective in heat transfer, with minimal effect on exhaust emissions of diesel engines. Most previous research has investigated liquid to liquid heat transfer in corrugated tubes at low Reynolds, not gas to liquid heat transfer. The SolidWorks Flow Simulation computer program was used to perform these studies.

The program is first validated by comparing simulation results with renowned correlations and field measurements. Simulations are then conducted for a concentric tube heat exchanger with corrugated tubes and twisted tapes of different configurations to determine the optimal design. The maximum enhancement in the rate of heat transfer was found in an annularly corrugated tube heat exchanger with twisted tape inserts. This exchanger transfers about 235.3 % and 67.26 % more heat compared to plain tube and annularly corrugated tube heat exchangers without twisted tapes, respectively. Based on optimal results, for a 120 kWe diesel generator, the application of an annularly corrugated tube heat exchanger with twisted tape inserts can save 2,250 gallons of fuel annually (a cost of approximately \$11,330) expected payback of initial cost in one month. In addition, saving heating fuel also reduces CO<sub>2</sub> emissions by 23 metric tons per year.

**Keywords:** Renewable energy; Corrugated tube; Twisted tapes; Exhaust gas; Heavy diesel generator; Waste heat recovery; Concentric tube heat exchanger.



## Table of Contents

	Page
Signature Page .....	i
Title Page .....	iii
Abstract .....	v
Table of Contents .....	ix
List of Figures .....	ix
List of Tables .....	xi
Acknowledgements .....	xiii
Chapter 1. Introduction .....	1
Chapter 2. Scope and Literature Review .....	3
2.1. Scope of the Work .....	3
2.2. Heat Exchangers .....	3
2.2.1. Shell and Tube Heat Exchangers .....	3
2.2.2. Straight Tube Heat Exchangers .....	4
2.2.3. U-tube Heat Exchangers .....	4
2.2.4. Concentric Tube Heat Exchangers .....	4
2.3. Corrugated Tube Heat Exchanger .....	6
2.4. Corrugated Tube Heat Exchanger with Twisted Tape inserts .....	7
2.5. Corrugated Tube Heat Exchanger with Modified Twisted Tape Inserts .....	8
Chapter 3. Mathematical Modelling & Validation .....	11
3.1. Governing Equations .....	11
3.2. Simulation Procedure .....	14
3.3. Mesh Independent Study .....	14
3.4. Validation .....	15
3.4.1. Using Existing Correlations .....	15
3.4.2. Using Field Measurement Results .....	17
3.5. Diesel Exhaust Heat Recovery System .....	18
3.5.1. Currently Installed System .....	18

3.5.2. Annularly Corrugated Tube Heat Exchanger Simulations .....	20
3.6. Proposed System to Improve Heat Transfer Performance .....	21
Chapter 4. Exhaust Heat Recovery with Helically Corrugated Tube Heat Exchangers.....	23
4.1. Effectiveness ( $\epsilon$ ) of ACT and HCT Heat Exchangers.....	26
4.2. Simulations of Helically Corrugated Tube Heat Exchangers.....	27
4.3. Discussion of Results.....	28
Chapter 5. Annularly Corrugated Tube Heat Exchanger with Twisted Tape Inserts .....	29
5.1. Simulations of the PTHE with Twisted Tapes .....	33
5.2. Simulations of ACT Heat Exchangers with Twisted Tapes (TT1, TT2, TT3 and TT4) .....	34
5.3. Effectiveness ( $\epsilon$ ) of PT and ACT Heat Exchangers .....	40
5.4. Economic Analysis .....	41
5.5. Discussion of Results.....	42
Chapter 6. Annularly Corrugated Tube Heat Exchanger with Modified Twisted Tape Inserts .....	45
6.1. Simulations of ACT Heat Exchanger with Modified Twisted Tapes.....	45
6.2. Simulations of ACT Heat Exchanger with Rod Twisted Tape (RTT) .....	47
6.3. Effectiveness ( $\epsilon$ ) of ACT Heat Exchangers with TT1 and Rod TT (D= 0.04m).....	50
6.4. Discussion of Results.....	51
Chapter 7. Conclusions .....	53
References.....	55

## List of Figures

Figure 1: Straight tube heat exchanger. ....	4
Figure 2: U-tube heat exchanger. ....	5
Figure 3: Concentric tube heat exchanger types. ....	5
Figure 4: Temperature profile of the gas at the tube exit for all the mesh sizes tested. ....	15
Figure 5: Heat exchanger used for validation, dimensions are in meters. ....	16
Figure 6: Reynolds number versus Nusselt number plot to compare simulation data with existing correlations for exhaust gas. ....	16
Figure 7: Schematic diagram of the current heat recovery system. ....	19
Figure 8: Exhaust heat recovery unit. ....	21
Figure 9: Classification of corrugated tubes. ....	23
Figure 10: Helically corrugated tube with a circular corrugation profile (HCT-1), a semicircular corrugation profile (HCT-2), and a V-shaped corrugation profile (HCT-3). ....	24
Figure 11: Cross-sectional view of (A) ACT heat exchanger; (B) HCT-2 heat exchanger. ....	25
Figure 12: Reynolds number versus heat transfer rate for HCT heat exchangers. ....	26
Figure 13: Flow trajectories with temperature distribution of the gas inside the ACT. ....	27
Figure 14: Flow trajectories with temperature distribution of the gas inside the HCT2. ....	28
Figure 15: Twisted tape dimensions. ....	29
Figure 16: Cross-sectional view of (A) ACT heat exchanger and (B) ACT heat exchanger with twisted tape. ....	32
Figure 17: Designed 3D model of twisted tape swirl generator. ....	33
Figure 18: Nu versus Re for tubes with different twisted tape inserts. ....	34
Figure 19: Twisted tape pitch versus enhancement percentage. ....	36
Figure 20: Flow trajectories with temperature distribution of gas inside a plain tube. ....	37
Figure 21: Flow trajectories with temperature distribution of gas inside an ACT. ....	37
Figure 22: Flow trajectories and temperature distribution of gas inside a PT with TT1. ....	38
Figure 23: Flow trajectories and temperature distribution of gas inside an ACT with TT1. ....	38
Figure 24: Velocity vectors inside an ACT and an ACT with TT1 at tube exit. ....	38



Figure 25: Heat transfer rate versus pitch of the twisted tape inserts in the ACTHE and PTHE.	39
Figure 26: Nusselt number versus Reynolds number for ACT and ACT with TTs. ....	40
Figure 27: Tangential velocity contour plot at exit of PTHE without and with TT (1-4) .....	44
Figure 28: Tangential velocity contour plot at the exit of an ACTHE without and with TT (1-4)... .....	44
Figure 29: Modified twisted tape inserts. ....	46
Figure 30: Nusselt number versus Reynolds number for ACT and ACT with modified TTs.....	47
Figure 31: Modified twisted tape inserts with rods: A) RTT1; B) RTT2; C) RTT3. ....	48
Figure 32: Heat recovery rate versus pressure drop of ACTHE with rod TTs. ....	49
Figure 33: Reynolds number versus Nusselt number for ACTHE with TT1 and RTT1.....	50

## List of Tables

Table 1: Corrugated tube dimensional details .....	19
Table 2: Plain tube and corrugated tube heat exchanger at $Re = 70,000$ .....	20
Table 3: Helically corrugated tube-related studies from the literature .....	24
Table 4: Comparisons for heat transfer rate and effectiveness .....	27
Table 5: Dimensional details of various twisted tapes.....	29
Table 6: Twisted tape insertions-related studies from the literature.....	30
Table 7: Heat transfer comparison for PTHE with TTs at a Reynolds number of 67,000 .....	34
Table 8: Simulation results of ACT heat exchanger with twisted tapes at $Re = 77,700$ .....	35
Table 9: Simulation results of ACT heat exchanger with twisted tapes at $Re = 66,200$ .....	35
Table 10: Simulation results of ACT heat exchanger with twisted tapes at $Re = 53,000$ .....	35
Table 11: Simulation results of ACT heat exchanger with twisted tapes at $Re = 40,000$ .....	35
Table 12: Heat exchanger effectiveness comparison.....	41
Table 13: Economic analysis .....	42
Table 14: Heat exchanger effectiveness .....	49



## Nomenclature

$C_p$	specific heat, J/kg K	$\rho$	density, kg/m <sup>3</sup>
$d$	tube diameter, m	$\mu_b$	viscosity, kg/m s
$d_t$	twisted tape diameter, m	$\mu_t$	eddy viscosity, kg/m s
$e$	enhancement	$\delta$	Kronecker delta
$f$	Darcy friction factor	$\vartheta$	viscous stress tensor
$h$	heat transfer coefficient, W/m <sup>2</sup> K	$\tau$	Reynolds stress tensor
$H$	total enthalpy, J	<i>Subscripts</i>	
$k$	turbulent kinetic energy, m <sup>2</sup> /s <sup>2</sup> , thermal conductivity, W/m K	$c$	cold fluid
$\dot{m}$	mass flow rate, kg/s	$h$	hot fluid
$Nu$	Nusselt number	$l$	laminar
$P_t$	twisted tape pitch, m	$t$	turbulent
$p$	pressure, kg/m s <sup>2</sup>	<i>Superscripts</i>	
$Pr$	Prandtl number	( $\bar{\quad}$ )	Reynolds average, average
$Q$	heat transfer rate, W	( $\tilde{\quad}$ )	Favre average
$q$	heat flux, W/m <sup>2</sup>	( $'$ )	Reynolds fluctuation
$Re$	Reynolds number	( $''$ )	Favre fluctuation
$T$	Temperature, K, Constant Time Interval, s	<i>Abbreviations</i>	
$t$	time, s	$ACT$	Annularly Corrugated Tube
$U$	quantity of parameters (e.g. velocity)	$CW$	Corrugation Width
$v, u$	fluid velocity, m/s	$HE$	Heat Exchanger
$x_i, x_j$	cartesian co-ordinates, m	$ID$	Inner Diameter
<i>Greek symbols</i>		$OD$	Outer Diameter
$\varepsilon$	effectiveness	$PT$	Plain Tube
$\varepsilon$	dissipation, m <sup>2</sup> /s <sup>3</sup>	$RTT$	Rod Twisted Tape
		$TT$	Twisted Tape



## Acknowledgements

I take it as a great pleasure to express my heartfelt thanks to my principal advisor, Dr. Chuen-Sen Lin, for his constant support, encouragement, and invaluable guidance during this research. I would also like to thank my advisory committee members, Dr. Debendra K. Das and Dr. Sun Woo Kim, for their valuable suggestions in completing the thesis.

I gratefully acknowledge financial support from the Department of Mechanical Engineering and the Alaska Center for Energy and Power.

I remain grateful to my parents, Mr. Anjaneya Prasad Mokkalpati and Mrs. Gayathri Devi Mokkalpati, and my sister, Ms. Pushkala Mokkalpati, on whose constant encouragement and love I have relied throughout my entire time at the University. Finally, I would like to thank my friends for their support and comments about my work.



## Chapter 1. Introduction

As fossil fuel reserves all over the world diminish, researchers seek to streamline existing energy sources and develop engines based on alternative energy sources. A major electricity source for the world is diesel engine power generators, which are used particularly in rural areas, for example, rural Alaska.

The heat dissipated into the atmosphere by diesel generator exhaust can amount to about one third of the fuel energy used. Normally, part of this heat can be captured with heat exchanger (HEs), then used to meet community heating and power needs. Plate heat exchangers are proven to be highly efficient, but are not used for exhaust heat recovery applications due to the pressure drop, potential soot accumulation, and high maintenance costs. Shell and tube and concentric tube type HEs are also used extensively. Their low-maintenance design makes this type of HEs an ideal solution for exhaust heat recovery.

In Alaska, about 180 villages have been using independent off-grid diesel generators for many decades. These generators are not equipped with exhaust heat recovery systems. Even a fraction of heat energy recovered may have a significant impact on heating fuel costs for villages in cold regions. From a village power industry point of view, the major reason for not installing exhaust heat recovery systems is maintenance difficulties resulting from soot accumulation and corrosion. In most of the villages, maintenance technicians and engineers are not readily available (especially during winters), and shipping equipment and travelling are also very expensive.

One of the heat recovery systems which can meet village needs is a vertically installed concentric tube heat exchanger. This design, when tested to capture the exhaust heat on a 120 kWe diesel generator, shows no evidence of emissions and maintenance problems. The heat exchanger is installed vertically in order to reduce soot accumulation. The water exiting the engine jacket is further heated in the current exhaust heat recovery system and supplied for space



heating. The advantages of using jacket water for heat recovery are economical installation, no additional pumping power required, and no extra loop cost.

The purpose of this work is to further improve the effectiveness of heat recovery using heat augmentation techniques. A literature review has been conducted on concentric tube heat exchangers to determine the most effective type of heat exchanger for cold region villages (Chapter 2). Heat transfer augmentation techniques are classified into active and passive methods. Active methods require direct external power, whereas passive methods do not. There are various techniques to reduce the thermal boundary layer thickness by improving mixing of the fluids near the walls and the center of the tube. Swirl flow generating devices provide chaotic mixing of the fluid and are a good passive method of heat transfer augmentation.

The exhaust heat recovery system currently being installed in Ruby, Alaska is a vertical concentric tube heat exchanger with a corrugated tube. To improve the effectiveness of the heat exchanger, heat transfer augmentation techniques discussed earlier will be adopted. Some of the effective possibilities to obtain the chaotic mixture of the fluid without an external power source are as follows:

1. Replacing the annularly corrugated tube with a helically corrugated tube.
2. Introducing twisted tape inserts in the annularly corrugated tube.
3. Introducing modified twisted tape inserts.

## Chapter 2. Scope and Literature Review

### 2.1. Scope of the Work

Extensive research has been done on liquid to liquid heat exchangers with corrugated tubes and plain tube concentric heat exchangers with twisted tape inserts for augmentation of heat recovery in various applications.

Researchers conducted experiments and numerical simulations on various concentric tube heat exchangers with a wide range of corrugated tube and twisted tapes individually and proved that they increase thermodynamic efficiency. Heat transfer applications like waste heat recovery methods, refrigeration, and air conditioning systems are using this type of swirl generators to enhance heat recovery. These studies are presented in the later sections of this chapter.

Promoting the swirl by the combined effect of corrugations and twisted tape for gas to liquid heat recovery applications (like diesel engine exhaust to water heat exchangers) is expected to be beneficial.

### 2.2. Heat Exchangers

Heat exchangers are devices used to transfer heat from one fluid to another fluid separated by a solid wall. There are several types of heat exchangers for different heat transfer applications. Some of them are discussed in this section, in order to select the most suitable heat exchanger for diesel engine exhaust heat recovery application.

#### *2.2.1. Shell and Tube Heat Exchangers*

Shell and tube HEs are typically used in oil refineries and many other industrial processes. This type of HEs consists of bundles of tubes inside a shell. Most of the time, the hot fluid circulates in the tube and cold fluid outside the tube to minimize the heat lost to the environment through the shell. Some shell and tube HE designs allow the hot fluid to flow through the shell to address soot accumulation concerns. There are many types of shell and tube HEs. The most commonly used are categorized as follows.

### 2.2.2. Straight Tube Heat Exchangers

Straight tube HEs' ends are connected to compartments of fluid entering and leaving. As the name indicates, the tubes are straight throughout the heat exchanger. Most shell and tube heat exchangers are one-pass, two-pass, or four-pass. "Pass" refers to the total number of times the warm fluid circulating tubes are allowed to pass through the cold fluid outside the tubes.

### 2.2.3. U-tube Heat Exchangers

For these HEs, the inlet and outlet are on the same side of the shell. As the name indicates, the tubes are U-shaped to provide more surface area in a single pass.

### 2.2.4. Concentric Tube Heat Exchangers

The major advantages of concentric tube HEs over shell and tube HEs are low initial cost and less maintenance required for both heat transfer surfaces, which is an important advantage especially for corrosive or soot-forming fluids. Engine back pressure drop, which may not be a significant factor for both HEs, is much lower in the case of concentric heat exchangers than shell and tube HEs. The disadvantages of this type of HEs in comparison with shell and tube HEs are low total heat transfer density and low absorption effectiveness. Figures 1 and 2 show the most common types of straight tube and U-tube heat exchangers.

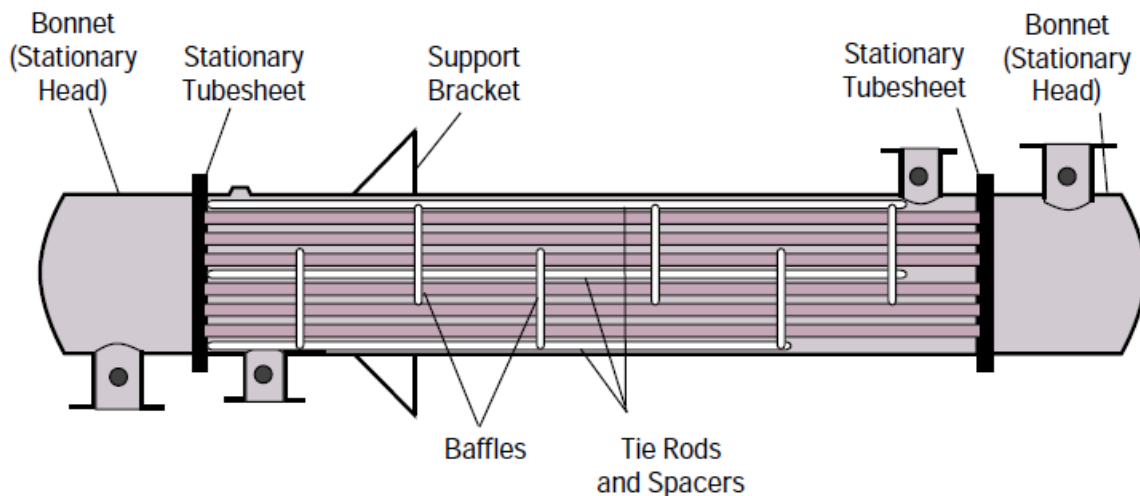


Figure 1: Straight tube heat exchanger.

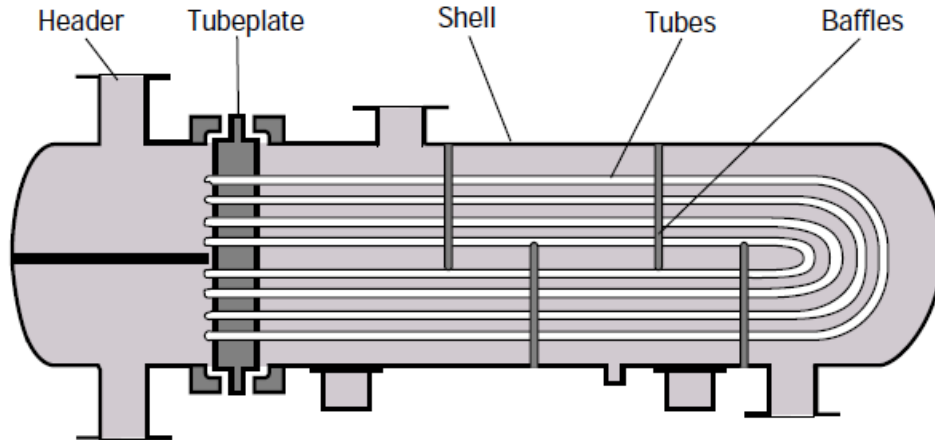


Figure 2: U-tube heat exchanger.

For industrial applications, there are many types of seamless pipes which can be used for concentric tube heat exchangers. Plain tubes and corrugated tubes are widely used in heat transfer applications. Figure 3 shows the parallel flow and counter-flow arrangement of a concentric tube heat exchanger.

Corrugated metal pipes have been extensively used in flood control, sewer systems, and other purposes, mostly other than heat transferring. Development is underway to improve their heat transfer performance along with size reduction.

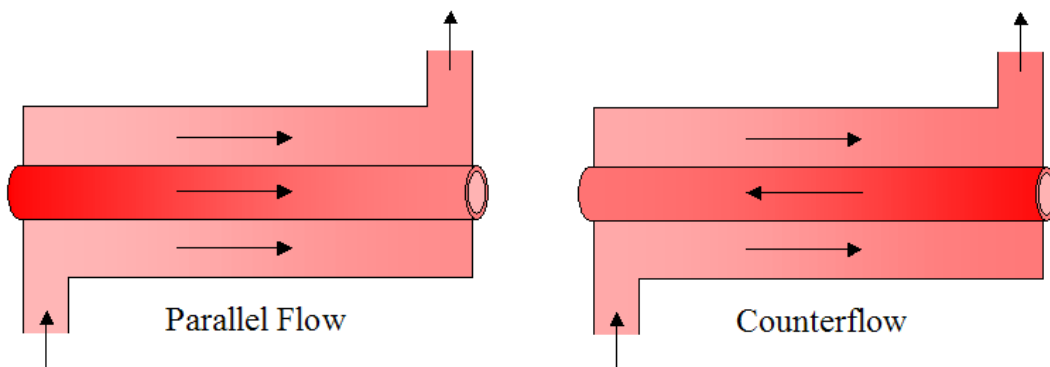


Figure 3: Concentric tube heat exchanger types.

Most of the power plants in rural Alaska use diesel engines for power and also significant amounts of fuel oil for heat. Recovering the waste heat from the exhaust and utilizing it for space heating and domestic water heating can improve fuel efficiency. For the cases where easy installation, easy maintenance, quick payback period, and availability of components are major concerns, concentric tube HEs can be one of the solutions.

### 2.3. Corrugated Tube Heat Exchanger

Withers [1] conducted an experimental investigation of the tube side behavior of various tubes with turbulent flow. Water was used as a working fluid and correlations were obtained to optimize the tube geometry for various applications. Withers found that the corrugated tubes enabled heat transfer enhancement ratios up to three times those of plain tubes.

Wang and others [2] investigated the heat transfer in carbon-copper/steel spirally fluted tubes. The heat transfer coefficient for spirally fluted copper tubes was up to 52% greater than that of plain copper tubes. Vicente and others [3] reported the isothermal friction and heat transfer characteristics of corrugated tubes with various geometries and also reported that the Nusselt's number and friction factor coefficient for their corrugated tubes were around 250% to 300% higher than those of the plain tube.

Pethkool and others [4] studied turbulent heat transfer enhancement in a heat exchanger using helically corrugated tubes with water as a working fluid. They found a mean increase in heat transfer rate between 123% and 232% compared to the plain tube. Ağra and others [5] investigated corrugated tubes and reported a higher heat transfer coefficient than that of plain tubes but a lower heat transfer coefficient than that of helically finned tubes.

García and others [6] experimental study concluded that for Reynolds numbers lower than 200, plain tubes are recommended; for Reynolds numbers between 200 and 2000, wire coils are more advantageous; for Reynolds numbers higher than 2000, corrugated and dimpled tubes are recommended for higher heat transfer rates. Han and others [7] investigated outward convex corrugated tubes (both symmetric and asymmetric) and reported that an asymmetric corrugated tube exhibits 8-18% higher heat transfer performance than that of a symmetric corrugated tube.

Poredos and others [8] experimented with concentric tube counter-flow in an air to air heat exchanger using corrugated tubes. Compared to plain tubes, the convective heat transfer coefficient increased only in corrugated tubes with a corrugation ratio of less than 1.6, but the heat transfer was 65-90% greater for all considered corrugated tubes due to the increased heat transfer surface area. Mohammed and others [9] investigated the influence of geometrical parameters and forced convective heat transfer in transversely corrugated circular tubes and reported that the best overall enhancement of 30% was achieved at  $Re=5000$ , in which the relative height of roughness is 0.025.

#### 2.4. Corrugated Tube Heat Exchanger with Twisted Tape Inserts

Al-Fahed and others [10] conducted experiments using oil as the working fluid for plain, microfin, and twisted tape insert tubes and concluded that the heat transfer is increased with the increase in the twist ratio. Saha and others [11] investigated the effect of regularly spaced twisted tape elements in laminar and turbulent flow regimes and reported that they increase heat transfer by 20-40%.

Ray and Date [12] conducted numerical analysis on inserting a twisted tape in a square duct and developed correlations for friction factor and Nusselt number and reported a fair agreement between the simulation and the experimental results. Garcia and others [13] conducted an experimental study on heat transfer in a plain tube with wire coil inserts in laminar-transition-turbulent regimes and stated that the heat transfer rate can be increased by up to 200%, keeping pumping power constant.

Eiamsa-ard and others [14] reported that the Nusselt number is increased by 160% using full length twisted tape and 179% by inserting helical tape with and without rods [15] inside the tube when compared with the plain tube. Naphon and Sriromrulk [16] conducted experiments by inserting the coiled wire in the plain tube and found that there is a significant effect of swirl in enhancing the rate of heat transfer.

Chang and others [17] investigated heat transfer in a tube with broken twisted tape inserts and reported that the thermal performance improved by up to 0.9-1.8 times that of tubes fitted

with plain twisted tape. Promvonge and Eiamsa-ard [18] investigated heat transfer behavior with conical ring and twisted tape inserts; they reported a 367% enhancement in heat transfer over a plain tube.

Promvonge [19] found that enhancement in heat transfer is about 1.2-1.3 times greater when a square wire coil is inserted in a circular tube. Promvonge [20] also conducted experiments to investigate air flow friction and heat transfer characteristics in a round tube fitted with both coiled wire and twisted tape and obtained 200-350% enhancement in heat transfer when compared to the plain tube.

Bharadwaj and others [21] conducted experiments using a spirally grooved tube with twisted tape inserts and reported 140% heat transfer enhancement over a plain tube. Rahimi and others [22] also conducted numerical simulations with various twisted tapes; compared with the classic twisted tape, they observed 31% enhancement in the heat transfer coefficient. Eiamsa-ard and others [23] performed numerical simulations of swirling flow in a circular tube by means of twisted tapes and reported that the mean heat transfer rates are about 73.6% higher than those of a plain tube.

Instead of changing the type of swirl generating device, Thianpong and others [24] changed the tube type, using a dimpled tube with classic twisted tape and found a heat transfer enhancement up to 1.66 to 3.03 times that of a plain tube. Similarly, inserting twisted tapes into a corrugated tube is expected to generate more swirl than in a plain tube, and also improve the rate of heat transfer.

## 2.5. Corrugated Tube Heat Exchanger with Modified Twisted Tape Inserts

Much recent research has involved twisted tape inserts with minor modifications. A few of these studies are discussed in this section. Chang and others [25] investigated the thermal performance of enhanced smooth and spiky twisted tapes for laminar and turbulent tubular flows and developed correlations for air to air heat exchangers. Eiamsa-ard and Seemawute [26] studied decaying swirl flow generated by short length twisted tapes and reported that the tapes with a smaller twist ratio gave higher heat transfer rates than the ones with a larger twist ratio, as

a result of stronger swirling flow at the entry. Their results show that the classic twisted tape has a greater heat transfer coefficient than that of short twisted tapes.

Chompookham and others [27] investigated heat transfer augmentation in a helical-ribbed tube with double twisted tape inserts and reported that, depending on twist ratios, this combination shows a substantial enhancement of heat transfer rate and thermal performance relative to a plain tube or a helical-ribbed tube alone. Bhuiya and others [28] investigated heat transfer and friction factor characteristics in turbulent flow through a tube fitted with perforated twisted tape inserts and reported an enhancement in rate of heat transfer when compared to a plain tube. Eiamsa-ard and others [29] studied the heat transfer enhancement by inserting uniform and non-uniform twisted tapes with alternate axes into a tube, and found that twisted tapes with the smaller alternate lengths give higher heat transfer rates than those with larger alternate lengths.

From the literature review, it is clear that generating swirl can improve the rate of heat transfer in a tube. Swirl can be produced in the tube by providing helical corrugations or by inserting twisted tape (classical or modified). To estimate the enhancement in terms of heat transfer at various swirl frequencies, helical corrugated tubes and twisted tapes are designed and a simulation performed.

SolidWorks Flow Simulation software is used to conduct a numerical study of the effect of swirl generated by twisted tapes of various configurations in corrugated tube heat exchangers. This program is first verified with known values of the heat transfer coefficient in highly turbulent flow regimes. A fair agreement of about  $\pm 10\%$  between the simulation results and correlation predictions [30] is observed. The simulation is then applied to a diesel engine exhaust gas to liquid heat exchanger. Based on the literature search, this is the first study of this type of gas to liquid heat exchanger.





## Chapter 3. Mathematical Modeling & Validation

The main goal of the simulations is to predict the relationship between heat transfer and the swirling of fluid inside heat exchanger tubes. Simulations are also performed for plain tube heat exchangers with similar conditions for reference. Assumptions and boundary conditions considered for all the simulations are listed below:

1. Steady operating conditions exist.
2. Radiation effects are much less than convection effects, and hence, are not included in the analysis.
3. Nitrogen gas is used in the simulations in place of exhaust gas, since it has similar thermal properties. It is treated as an ideal gas.
4. The ambient pressure and the pressure at exit are both assumed to be 1 atmosphere (atm).
5. The ambient temperature is assumed to be 20°C, with a heat transfer coefficient of 15 W/m<sup>2</sup>K.
6. The inlet volume flow rate and temperature of water are 0.00397 m<sup>3</sup>/s (63 gpm) and 90.55°C, respectively.
7. The inlet volume flow rates of exhaust are 0.3933 m<sup>3</sup>/s, 0.3343 m<sup>3</sup>/s, 0.2753 m<sup>3</sup>/s, and 0.1966 m<sup>3</sup>/s, in order to estimate the trend over a range. The temperature of the engine exhaust is 510°C.
8. The heat exchanger is installed vertically.

### 3.1. Governing Equations

SolidWorks software performs the numerical analysis. The Favre Averaged Navier Stokes (FANS) equations are used in this CFD package to model velocity and pressure fields. These equations include the laws of conservations of mass, momentum, and energy for three-dimensional models, and are also suitable for highly turbulent flow cases [31], which is density-weighted, time-averaging Navier Stokes equation.

Most computational fluid dynamics software (e.g., ANSYS, FLUENT, etc.) uses the Reynolds average Navier Stokes equations. Favre averaging can also be used in compressible flow to distinguish turbulent fluctuations from the mean flow. In most uses, FANS is not necessary, since turbulent fluctuations do not always lead to any substantial fluctuations in density. In this case, the simpler RANS equations can be used. Only in highly compressible flows and hypersonic flows is it necessary to perform the more complex Favre averaging.

Equation 7 shows classical time averaging for density and pressure, known as Reynolds averaging:

$$\bar{U} = \lim_{T \rightarrow \infty} \frac{1}{T} \int_t^{t+T} U(t) dt \quad (7)$$

$$U = \bar{U} + U'$$

Equation 8 shows density-weighted time-averaging for velocity and energy, i.e., Favre averaging:

$$\tilde{U} = \frac{1}{\bar{\rho}} \lim_{T \rightarrow \infty} \frac{1}{T} \int_t^{t+T} \rho(t) U(t) dt \quad (8)$$

$$U = \tilde{U} + U''; T = \text{Constant Time interval}$$

The Favre Averaged Navier Stokes (FANS) [33] equations, i.e., conservation equations, can be written as follows.

Continuity equation:

$$\frac{\partial \bar{\rho}}{\partial t} + \frac{\partial (\bar{\rho} \tilde{u}_i)}{\partial x_i} = 0 \quad (9)$$

Momentum equation:

$$\frac{\partial (\bar{\rho} \tilde{u}_i)}{\partial t} + \frac{\partial}{\partial x_j} \left( (\bar{\rho} \tilde{u}_i \tilde{u}_j) + \bar{p} \delta_{ij} + \overline{\rho u_i'' u_j''} - \bar{\tau}_{ji} \right) = 0 \quad (10)$$

and Reynolds stress tensor:

$$\tau_{ij} = -\overline{\rho u_i'' u_j''} \quad (11)$$

Boussinesq equation expressing the Stress Tensor”

$$\tau_{ij} = \mu_t \left( \frac{\partial \tilde{u}_i}{\partial x_j} + \frac{\partial \tilde{u}_j}{\partial x_i} - \frac{2}{3} \frac{\partial \tilde{u}_k}{\partial x_k} \delta_{ij} \right) - \frac{2}{3} \bar{\rho} k \delta_{ij} \quad (12)$$

Total Enthalpy:

$$\frac{\partial}{\partial t} (\bar{\rho} H) + \frac{\partial}{\partial x_j} (\bar{\rho} \tilde{u}_j H) = \frac{\partial}{\partial x_j} \left[ -q_{lj} - q_{tj} + \overline{\vartheta_{ij} u_i''} - \overline{\rho u_j'' \frac{1}{2} u_i'' u_i''} \right] + \frac{\partial \bar{p}}{\partial t} + \frac{\partial}{\partial x_j} [\tilde{u}_i (\bar{\vartheta}_{ji} + \tau_{ji})] \quad (13)$$

$$\bar{p} = \bar{\rho} R \tilde{T}, \quad H = \tilde{h} + \frac{1}{2} \tilde{u}_i \tilde{u}_i + k, \quad k = \frac{1}{2} \overline{\rho u_i'' u_i''}$$

where  $H$  = Total enthalpy,  $\tilde{h}$  = Static enthalpy,  $k$  = turbulence kinetic energy,  $q_{lj}$  = Laminar heat flux vector, and  $q_{tj}$  = Turbulent heat flux vector. This study uses  $k$ - $\varepsilon$  turbulence model.

For turbulent kinetic energy ( $k$ ):

$$\frac{\partial \rho k}{\partial t} + \frac{\partial}{\partial x_i} (\rho u_i k) = \frac{\partial}{\partial x_i} \left( \left( \mu + \frac{\mu_t}{\sigma_k} \right) \frac{\partial k}{\partial x_i} \right) + \tau_{ij}^R \frac{\partial u_i}{\partial x_j} - \rho \varepsilon + \mu_t P_B, \quad (14)$$

For dissipation ( $\varepsilon$ ):

$$\frac{\partial \rho \varepsilon}{\partial t} + \frac{\partial}{\partial x_i} (\rho u_i \varepsilon) = \frac{\partial}{\partial x_i} \left( \left( \mu + \frac{\mu_t}{\sigma_\varepsilon} \right) \frac{\partial \varepsilon}{\partial x_i} \right) + C_{\varepsilon 1} \frac{\varepsilon}{k} \left( f_1 \tau_{ij}^R \frac{\partial u_i}{\partial x_j} + \mu_t C_B P_B \right) - C_{\varepsilon 2} f_2 \frac{\rho \varepsilon^2}{k} \quad (15)$$

$$f_1 = 1 + \left( \frac{0.05}{f_\mu} \right)^3, \quad f_2 = 1 - \exp(-R_T^2)$$

Turbulent viscosity factor ( $f_\mu$ ):

$$f_\mu = [1 - \exp(-0.025 R_y)]^2 \cdot \left( 1 + \frac{20.5}{R_T} \right) \quad (16)$$

$$R_T = \frac{\rho k^2}{\mu \varepsilon}, \quad R_y = \frac{\rho \sqrt{k} \cdot y}{\mu}$$

The constants  $C_\mu = 0.09, C_{\varepsilon_1} = 1.44, C_{\varepsilon_2} = 1.92, \sigma_\varepsilon = 1.3, \sigma_k = 1$  are defined empirically [31].

### 3.2. Simulation Procedure

The basic flow equations are derived in finite volume method using integral approach. The conservation equations are discretized and solved throughout the model. The rate of increase in the quantity is equal to the sum of difference in the flux quantity and generation:

$$\frac{\partial}{\partial t} \int_v U dV = - \oint_s \vec{F} \cdot d\vec{S} + \int_v Q dv \quad (17)$$

where  $U$  represents the quantity,  $V = \text{Volume}$ ,  $S = \text{Surface}$ ,  $F = \text{Flux}$  and  $Q = \text{Source}$ . The second order approximations of fluxes ( $F$ ) are based on modified Leonard's Quadratic Upstream Interpolation for Convective Kinetics (QUICK) approximations and the Total Variation Diminishing (TVD) method. The pressure velocity coupling numerical algorithm, i.e., Semi Implicit Method for Pressure Linked Equations (SIMPLE), is used to estimate the pressure field [31].

### 3.3. Mesh Independent Study

Three different meshes, with 387,705, 538,467, and 924,491 cells, are considered initially. A mesh independent study was performed to verify the results. The results of heat transfer rate and outlet temperatures are compared and the discrepancies between the results are less than 0.5% (Fig. 4). The intermediate mesh level is chosen for all the simulations, which reduces simulation time by 41.76% and gives similar results (0.5% deviation) to the very fine mesh.

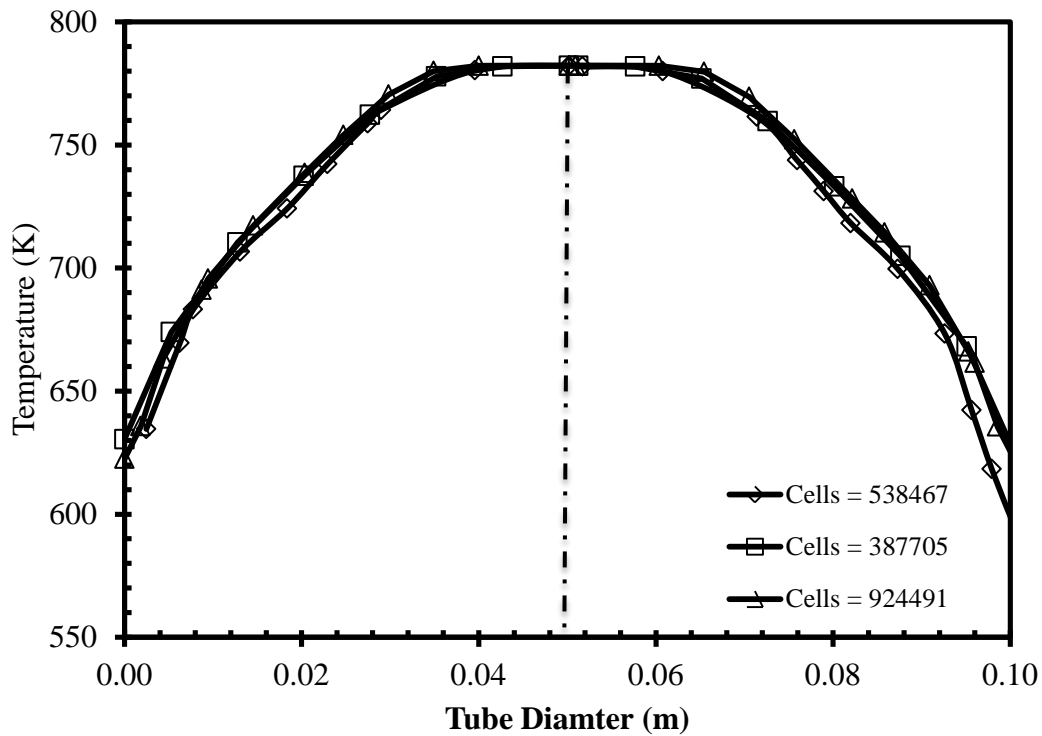


Figure 4: Temperature profile of the gas at the tube exit for all the mesh sizes tested.

### 3.4. Validation

#### 3.4.1. Using Existing Correlations

The numerical simulations are performed on a concentric tube heat exchanger (Fig. 5) to validate the heat transfer coefficient obtained from the simulation with the existing correlations for the Nusselt number. Nusselt number values obtained experimentally agree with those from the numerical analysis (less than 10% difference for the inner tube).

Figure 6 compares the numerical analysis, Dittous-Boelter's correlation, Gnielinski's correlation, and Petukhov's correlation [32] in terms of the dimensionless parameters Nusselt number (Nu), Reynolds number (Re), and Prandtl number (Pr).

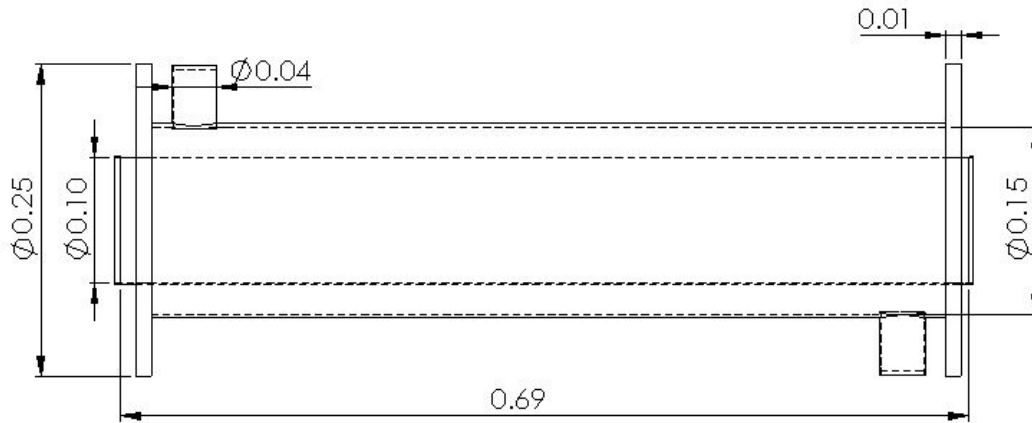


Figure 5: Heat exchanger used for validation, dimensions are in meters.

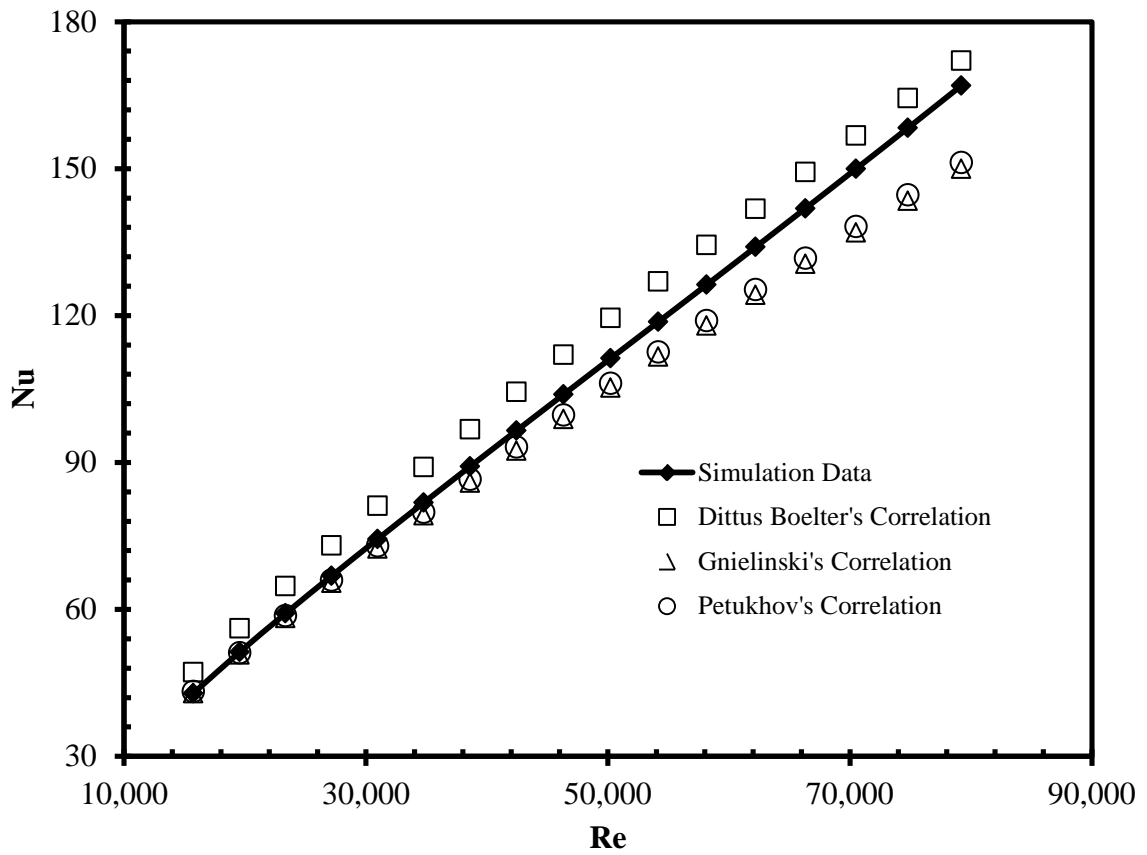


Figure 6: Reynolds number versus Nusselt number plot to compare simulation data with existing correlations for exhaust gas.

Nusselt number

$$Nu = hd_h/k \quad (18)$$

Reynolds number

$$Re = \rho v d_h / \mu \quad (19)$$

Prandtl number

$$Pr = C_p \mu / k \quad (20)$$

Dittus-Boelter's correlation

$$Nu = 0.024 Re^{0.8} Pr^{0.3} \quad (21)$$

Gnielinski's correlation

$$Nu = \frac{(f/8)(Re-1000) Pr}{1+12.7(f/8)^{0.5}(Pr^{0.67}-1)} \quad (22)$$

where friction factor  $f$  in the above equation can be defined using Petukhov's correlation

$$f = (0.79 \ln(Re) - 1.64)^{-2}$$

Petukhov's correlation

$$Nu = \frac{(f/8) Re Pr}{C+12.7(f/8)^{0.5}(Pr^{0.67}-1)} \quad (23)$$

where constant  $C$  in the above equation can be defined as

$$C = 1.07 + 900/Re - [0.63/(1 + 10Pr)]$$

### 3.4.2. Using Field Measurement Results

According to the Ruby, Alaska power plant report, heat recovered by a 60/40 ethylene glycol/water mixture in an annularly corrugated concentric tube vertical heat exchanger with counter-flow is about 4.83 kW, the jacket water temperature was increased by 1.11°C. EG water (cold fluid) with a temperature of 90.55°C is flowing at 30 gpm (0.0012212 m<sup>3</sup>/s) between shell and tube, and exhaust gas (hot fluid) with a temperature of 412°C flowing inside the corrugated tube at the rate of 0.3146 m<sup>3</sup>/s.



Under similar conditions, the annularly corrugated concentric tube vertical heat exchanger is simulated, with counter-flow. The simulation results show a temperature increase of 1.56 °C and a heat recovery of 6.68 kW by the EG water, which is 27.7% more than that of the heat recovered by the EG water in the power plant. It is believed that uncertainties in the measuring devices used in the power plant and the approximations in the calculations and the simulation results are close enough for comparison between the field measurement results and simulation results.

### 3.5. Diesel Exhaust Heat Recovery System

#### *3.5.1. Currently Installed System*

The power plant in Ruby, Alaska currently uses a vertically installed concentric tube heat exchanger with an annularly corrugated inner tube for exhaust and a plain outer tube with jacket water which is exiting the diesel engine jacket to capture exhaust heat for space heating. This heat recovery system is attached to a John Deere G4045-T300-HF458 Tier 3, 2010 model year, 1800 RPM, 120 kWe diesel generator (Fig. 7) [34]. The installation is proved to be an inexpensive retrofit.

The annularly corrugated tube of the heat recovery unit installed in the Ruby power plant was manufactured by Penflex Corporation. The following drawings and dimensions are provided on request. Dimensional details are presented in Table 1.

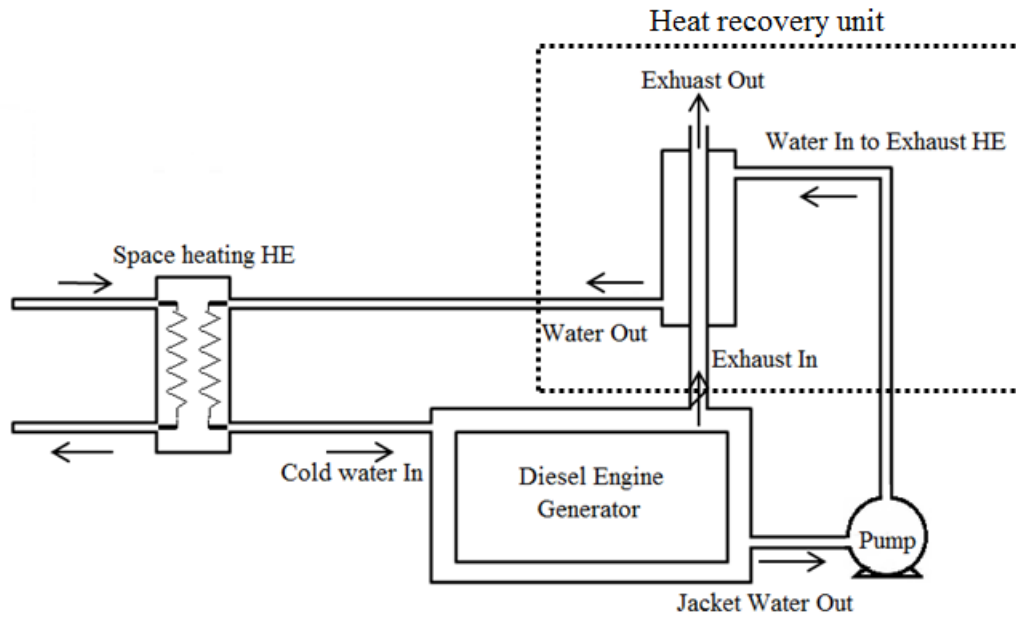


Figure 7: Schematic diagram of the current heat recovery system.

The dimensions of the outside tube (shell) and inside tube (ACT) of the heat recovery system are presented in Table 1 and Figure 8.

Table 1: Corrugated tube dimensional details

Tube	Pitch (m)	CW (m)	OD (m)	ID (m)	Thickness (m)
Plain	-	-	0.102	0.1016	$0.61 \times 10^{-3}$
Corrugated	0.0105	0.0075	0.122	0.1016	$0.61 \times 10^{-3}$

The corrugated tube has 2.69 times the heat transfer surface area than that of a plain tube, and hence can improve the rate of heat transfer.

### 3.5.2. Annularly Corrugated Tube Heat Exchanger Simulations

Simulations have been performed for the current heat exchanger with the flow conditions mentioned earlier in this chapter. The results are then compared with those of a plain tube heat exchanger of similar physical dimensions. The results and comparisons are presented in Table 2.

Table 2: Plain tube and corrugated tube heat exchanger at  $Re = 70,000$

Heat Exchanger	Surface Area (m <sup>2</sup> )	% increase	Heat Transfer (kW)	% Change
Plain Tube	0.225	-	6.8	-
Corrugated Tube	0.606	169	11.4	68.6

The previous heat recovery system was installed with a plain tube and then replaced by a corrugated tube of the same length. This increased the total heat transfer surface area by about 169%, which enhanced the rate of heat transfer up to 68% at a Reynolds number of 77,000. The simulations have been performed over a range of Reynolds numbers from 40,000 to 77,000. The results are discussed in later chapters.

The annularly corrugated tube improves the heat transfer surface area. If the fluid is provided with the swirling affect, the rate of heat transfer can be further improved. By replacing the annularly corrugated tube with a helically corrugated tube of similar surface area, the swirling effect of the fluid can be achieved, and thus the rates of heat transfer increased.

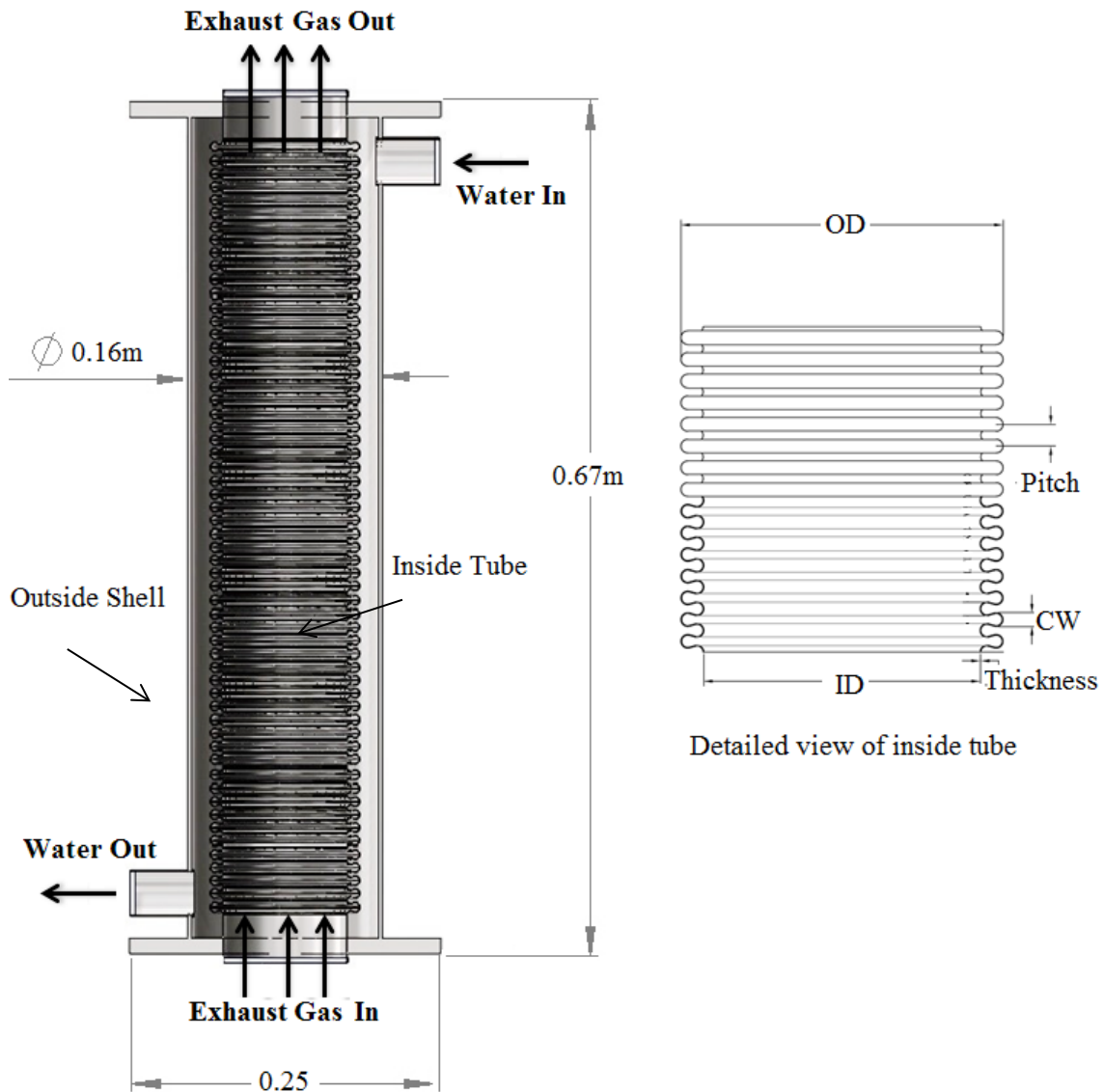


Figure 8: Exhaust heat recovery unit (Generated 3D model).

### 3.6. Proposed System to Improve Heat Transfer Performance

The goal of the present work is to maximize the heat recovery rate by optimizing the corrugated tube parameters or making minor modifications. The controlled variables include the

Reynolds number of the exhaust, which ranges from 40,000 to 77,000. The physical size of the heat exchanger and the exhaust back pressure change are the constraints.

## Chapter 4. Exhaust Heat Recovery with Helically Corrugated Tube Heat Exchangers

Helically corrugated tubes with very large diameters and lengths are commonly used in heating ventilation and air conditioning, civil, and sewer applications. This study uses corrugation profiles similar to those of the tubes used for these to investigate the advantages of incorporating helically corrugated tubes in the exhaust heat recovery applications.

Corrugated tubes can have annular or helical/spiral corrugation. Annular corrugation can improve the heat transfer surface area and helical corrugation can provide the swirling flow to the fluid, along with increased surface area. Helically corrugated tubes are subdivided into single start and multi-start. Multi-start corrugated tubes can provide more swirl than single start corrugated tubes. Figure 9 shows the complete classification of corrugated tubes.

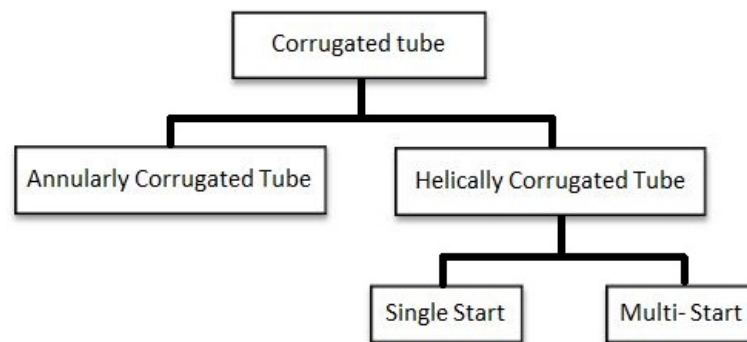


Figure 9: Classification of corrugated tubes.

Three different helically corrugated tubes with similar dimensions to those of an annularly corrugated tube are modeled and simulated in order to investigate the rate of heat transfer enhancement among them. The drawings developed using SolidWorks are presented in Figure 10. Table 3 provides a summary of the related work discussed in Chapter 2.

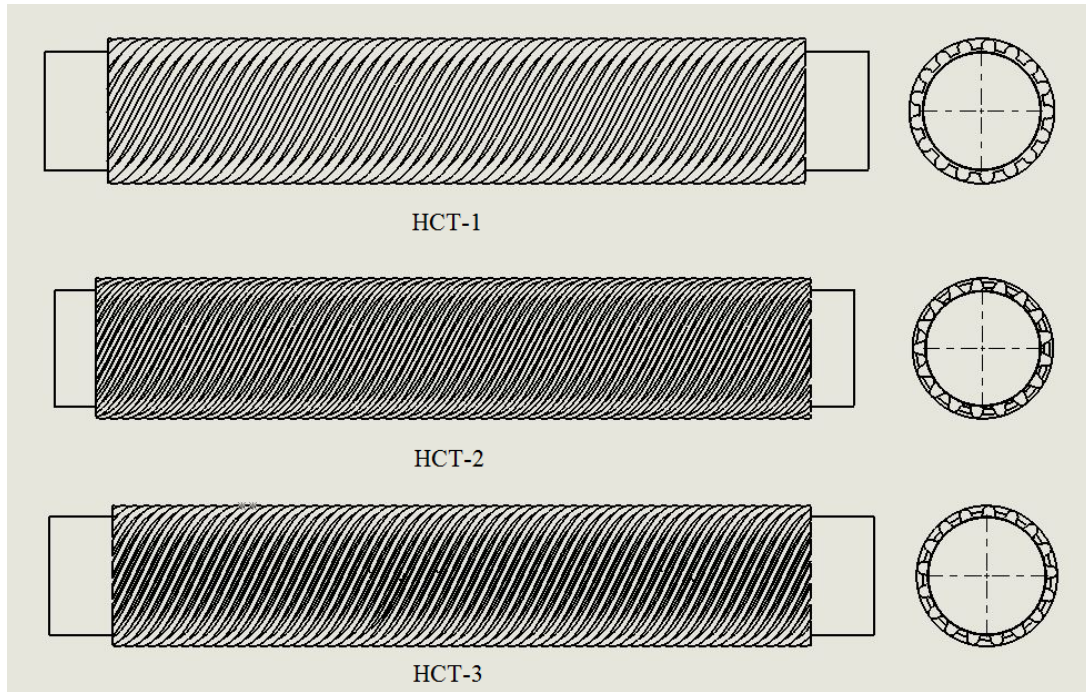


Figure 10: Helically corrugated tube with a circular corrugation profile (HCT-1), a semicircular corrugation profile (HCT-2), and a V-shaped corrugation profile (HCT-3).

Table 3: Helically corrugated tube-related studies from the literature

Paper	Tube	Diameter (m)	Fluid	Increase
James G. Withers	Single-helix corrugated tube	0.0158 – 0.0317	Water <sup>b</sup>	150-200%
L. Wang et al.	Spirally fluted tube	0.016	Steam <sup>c</sup>	10-17%
Vicente et al.	Corrugated tube	0.018	Water <sup>b</sup>	30% <sup>a</sup>
Pethkool et al.	Helically corrugated tube	0.0285	Water <sup>b</sup>	123-232%
P. Poredos et al.	Corrugated tubes	0.13 – 0.085	Air <sup>c</sup>	65-90%

Note: the citations reported are experimental investigations and arranged in chronological order.

<sup>a</sup> Laminar and turbulent flows, all other flows are turbulent regime;

<sup>b</sup> Liquid to liquid HE; <sup>c</sup> Gas to gas HE;

Figure 11 shows a cross-sectional view of helically corrugated tubes in a vertical heat exchanger. We performed numerical simulations for all the systems using the boundary conditions specified in the previous chapter. Table 4 and Figure 12 show simulation results.

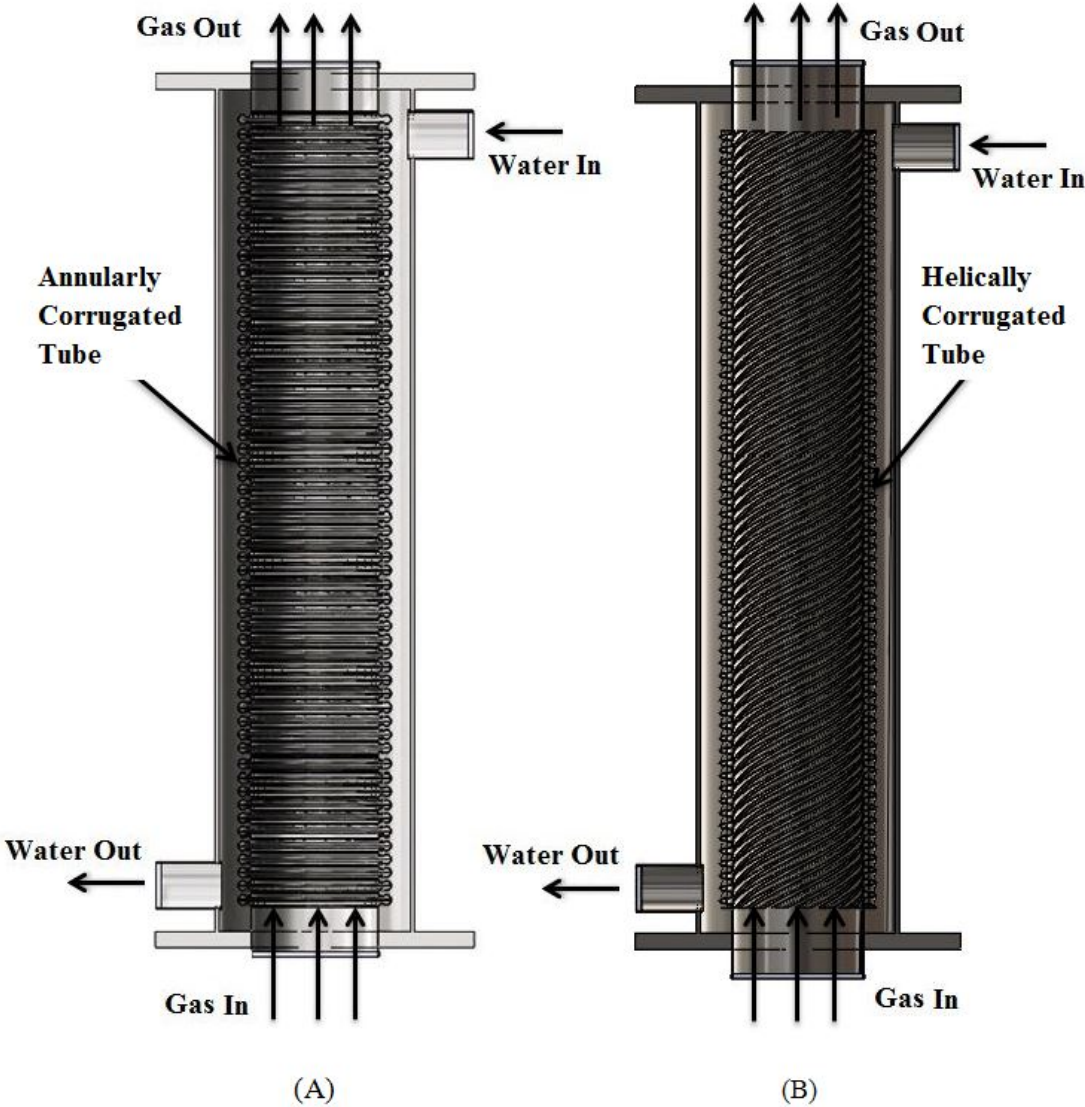


Figure 11: Cross-sectional view of (A) ACT heat exchanger; (B) HCT-2 heat exchanger.



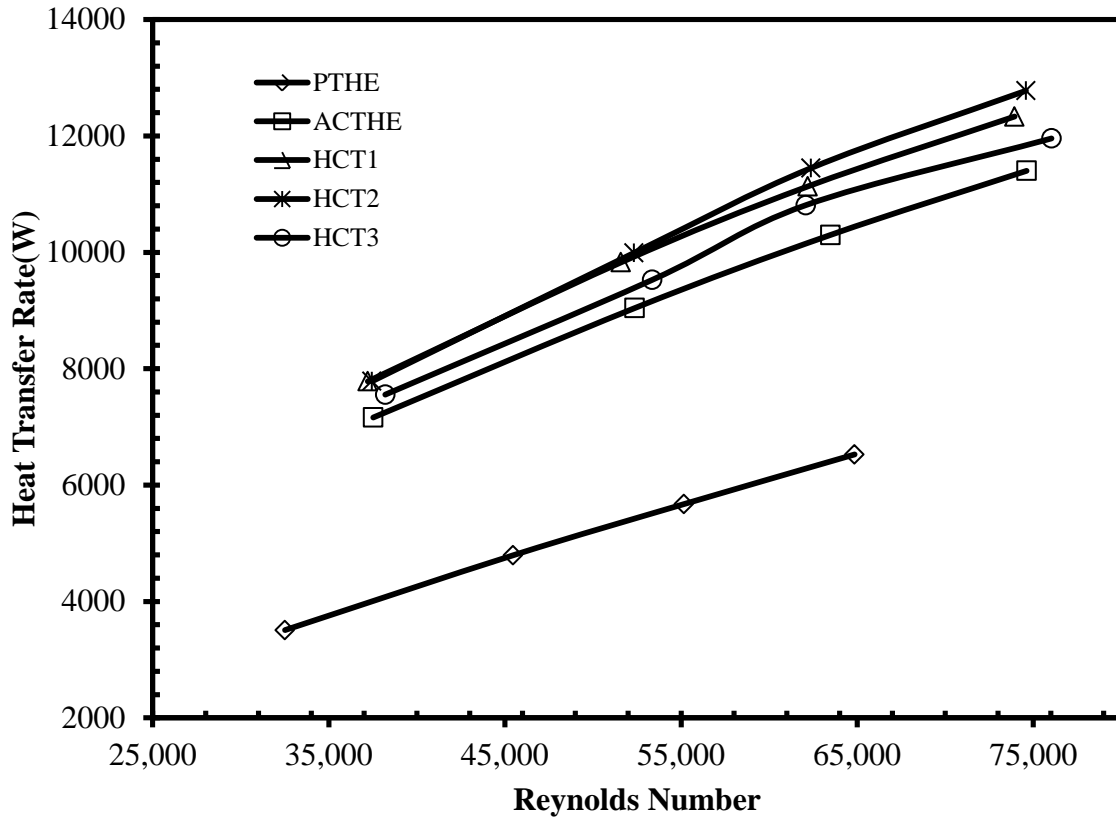


Figure 12: Reynolds number versus heat transfer rate for HCT heat exchangers.

#### 4.1. Effectiveness ( $\epsilon$ ) of ACT and HCT Heat Exchangers

Effectiveness is a measure of heat transfer performance of a heat exchanger and is denoted by  $\epsilon$ . The effectiveness of a heat exchanger can be defined as the ratio of the total amount of heat that has been exchanged to the maximum possible heat transfer rate [35].

$$\epsilon = \frac{Q}{Q_{max}} \quad (19)$$

$$\text{where } Q = C_c(T_{c,o} - T_{c,i}) = C_h(T_{h,i} - T_{h,o}); Q_{max} = C_{min}(T_{h,i} - T_{c,i})$$

$$C_c = \dot{m}_c c_p; C_h = \dot{m}_h c_p; C_{min} = \text{Minimum of } C_c \text{ and } C_h$$

## 4.2. Simulations of Helically Corrugated Tube Heat Exchangers

The total heat recovered by the water from exhaust gas is 12.11 kW, with a temperature increase of about 0.75°C. Figures 13 and 14 visualize the flow trajectories of the nitrogen gas inside the annularly corrugated tube and helically corrugated tube heat exchangers.

Table 4: Comparisons for heat transfer rate and effectiveness

Heat Exchanger	Heat Transfer rate(kW)	Effectiveness ( $\epsilon$ in %)	Enhancement (%)
ACT	11.47	14.34	-
HCT-1	12.33	15.48	7.9
HCT-2	12.78	16.05	11.9
HCT-3	11.9	15.01	3.8

The heat transfer rate in the above table is directly obtained from the CFD program and the effectiveness is calculated using basic equations.

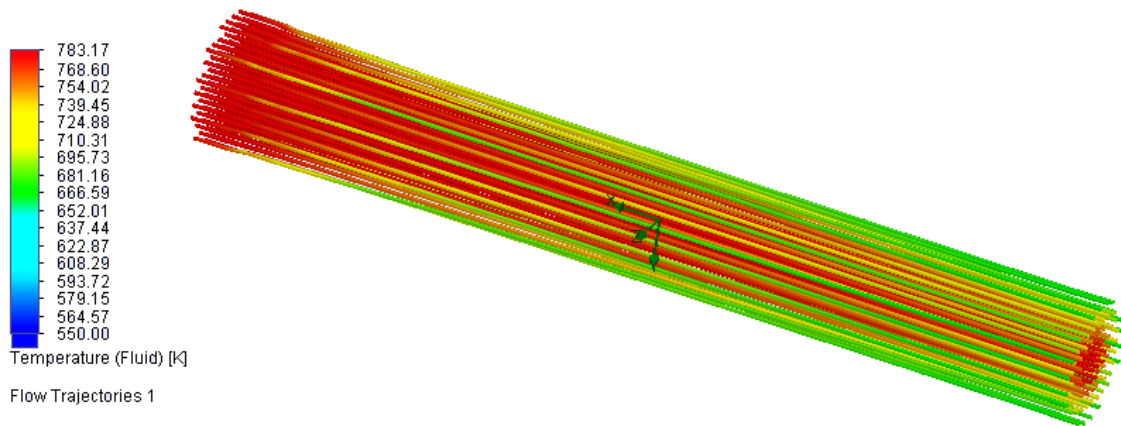


Figure 13: Flow trajectories with temperature distribution of the gas inside the ACT.

The presented values show a significant enhancement in the rate of heat transfer and the effectiveness of the heat exchanger by about 12.1% at a Reynolds number of about 77,000 when HCT-2 is used.

To support this argument, Figure 14 presents fluid flow trajectories of annularly corrugated and helically corrugated tubes, along with temperature distributions. The fluid shown in red represents the maximum temperature and the fluid shown in blue represents the minimum temperature. The temperature scale ranges from 783.15 K to 500 K.

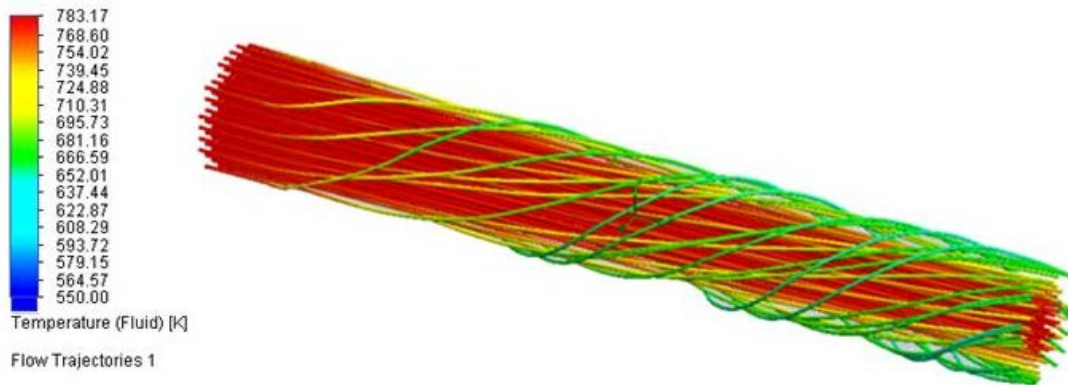


Figure 14: Flow trajectories with temperature distribution of the gas inside the HCT2.

#### 4.3. Discussion of Results

Simulation results show that, for the same heat exchanger dimension (i.e., height and diameter), the heat transfer rate of a helically corrugated tube heat exchanger (HCTHE) is about 12% higher than that of an annularly corrugated tube heat exchanger (ACTHE). The total heat transfer surface areas for all the designed HCTs are similar to that of the ACT.

It is believed that the swirl generated in the tube is responsible for the heat transfer enhancement, since all the other parameters (i.e., heat surface area, flow rates, and inlet temperatures of both the fluids) remain unchanged. HCT2 generates more swirls and hence recovers more heat than other tubes.

In order to select the optimal twisted tape insert, four different twisted tapes with different pitches are modeled and tested in the ACTHE (Table 5). Table 6 summarizes the literature review for heat exchangers with twisted tape inserts discussed in Chapter 2, Section 3.

Chapter 5. Annularly Corrugated Tube Heat Exchanger with Twisted Tape Inserts

Although a helically corrugated tube can recover about 12.1% more heat than an annularly corrugated tube, this tube is not readily available on the market. The manufacturing cost for HCTs can be cheaper only when they are produced on a large scale. To further improve the heat transfer rate of the heat recovery system, a modification of inserting a twisted tape into an existing corrugated tube heat exchanger is investigated.

The modifications need to be retrofittable, cost-effective, and have negligible effect on emissions, maintenance, and pumping power. Inserting twisted tapes in the present heat recovery system has an almost negligible effect on all the above aspects. The combined effect of the twisted tape and corrugations is expected to increase swirling of exhaust and also the rate of heat transfer. Figure 15 shows the dimensions of the twisted tape.

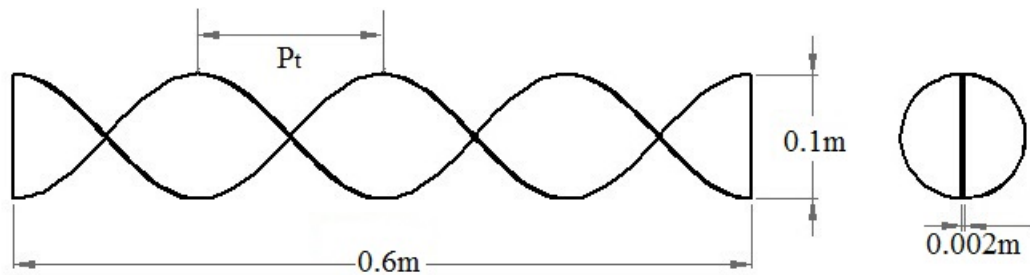


Figure 15: Twisted tape dimensions.

Table 5: Dimensional details of various twisted tapes

Twisted Tape(TT)	Pitch( $P_t$ )	$P_t/d_t$	Number of twists
TT1	0.15m	1.5	4
TT2	0.2m	2	3
TT3	0.25m	2.5	2.4
TT4	0.3m	3	2

Table 6: Twisted tape insertions-related studies from the literature

Paper	Tube	Tube diameter	Swirl generator	Working fluids	Increase
Al-Fahed et al.	Microfin tube	14mm	Twisted tape	Steam to oil <sup>c</sup>	225% <sup>a</sup>
Saha et al.	Plain tube	13mm	Spaced twisted tapes	Oil <sup>++</sup>	20-40% <sup>a</sup>
Ray and Date <sup>b</sup>	Square duct	9.5mm×9.5mm	Twisted tapes	Water <sup>f</sup>	-
Garcia et al.	Plain tube	18mm	Wire coils	PG Water <sup>c</sup>	200%
Eiamsa-ard et al.	Plain tube	19mm	Helical tape	Water to air <sup>e</sup>	160%
Naphon et al.	Microfin tube	8.92mm	Coiled wire inserts	Water <sup>c</sup>	~20%
Eiamsa-ard et al.	Plain tube	50mm	Spaced twisted tapes	Water <sup>c</sup>	179%
Chang et al.	Plain tube	20mm	Broken twisted tape	Air <sup>d</sup>	0.9-1.8 times
Promvongse et al.	Plain tube	48mm	Conical ring and twisted tape	Air <sup>d</sup>	367%
Promvongse	Plain tube	47.5mm	Coiled square wires	Air <sup>d</sup>	2.4 times
Promvongse	Plain tube	47mm	Wire coil & twisted tape	Air <sup>d</sup>	200-350%
Bharadwaj et al.	Grooved tube	14.8mm	Twisted tape	Water <sup>d</sup>	400% <sup>a</sup> , 140%
Rahimi et al. <sup>b</sup>	Plain tube	17mm	Modified twisted tapes	Water <sup>c</sup>	2.49-1.96 times
Eiamsa-ard et al. <sup>b</sup>	Plain tube	(2.5-5.0)×P	Loose fit twisted tapes	Water <sup>f</sup>	73.6%
Thianpong et al.	Dimpled tube	22mm	Twisted tape	Water <sup>c</sup>	1.66-3.03 times
Present study	Corrugated tube	101.5mm	Twisted tape	N <sub>2</sub> to water <sup>e</sup>	235.3%

Note: the citations reported are arranged in chronological order; <sup>a</sup>laminar flow, all other flows are under a turbulent regime; <sup>b</sup>numerical (CFD) study, all other reports are experimental investigations; <sup>c</sup>liquid to liquid HE; <sup>d</sup>electric heat source to liquid/gas HE; <sup>e</sup>gas to liquid HE; <sup>f</sup>constant heat flux boundary condition.



Figure 16 shows 3D models of the ACTHEs with and without twisted tapes.

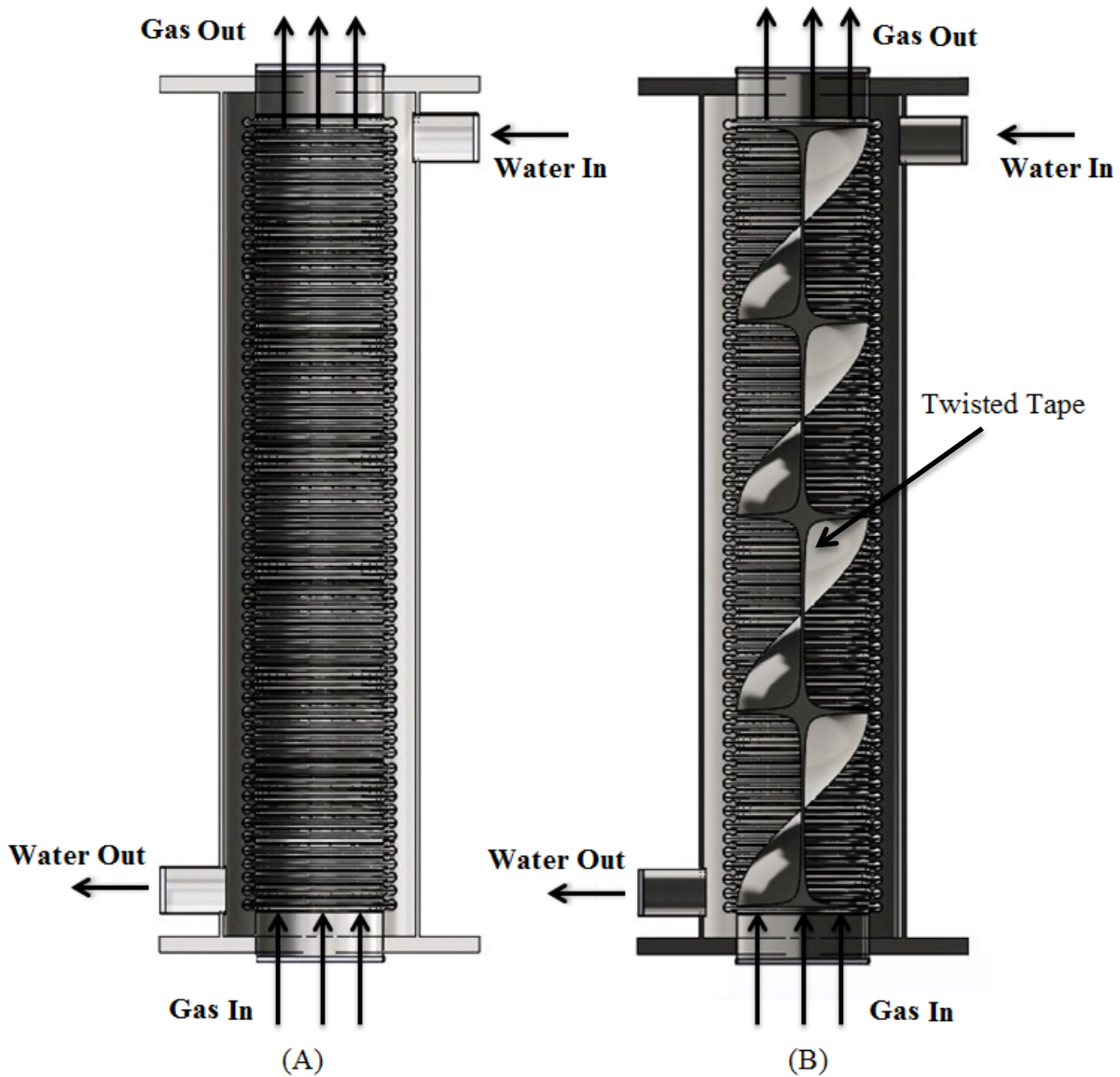


Figure 16: Cross-sectional view of (A) ACT heat exchanger and (B) ACT heat exchanger with twisted tape.

The pitch of the twisted tape is inversely proportional to the number of twists. In general, it is believed that the greater the number of twists, the more fluid swirl can be achieved. Too many twists may increase the manufacturing difficulty as well as the back pressure drop. Figure 17 presents a 3D model for visualization.

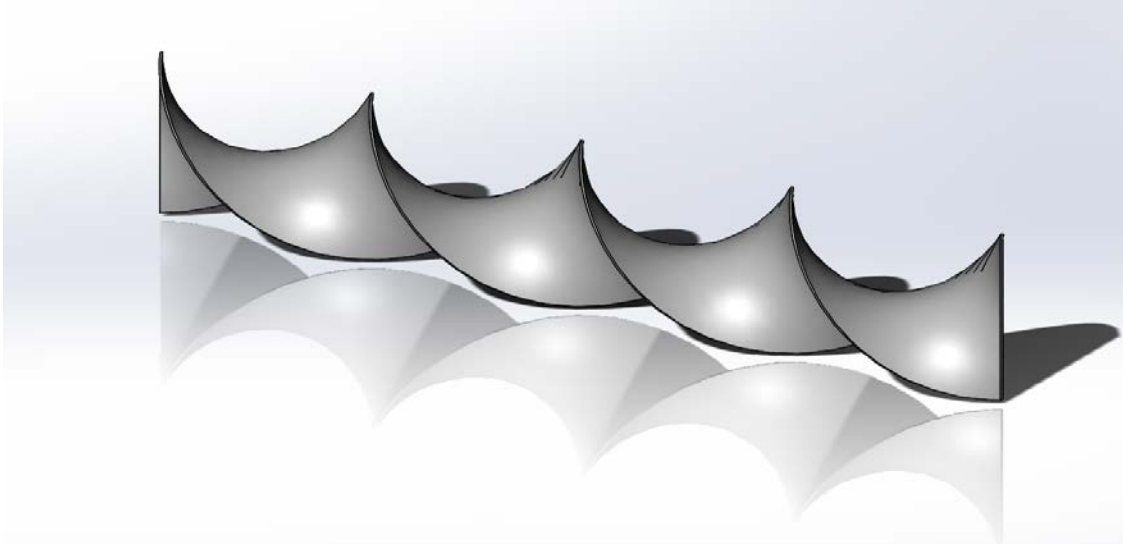


Figure 17: Designed 3D model of twisted tape swirl generator.

To design the optimal twisted tape for exhaust heat recovery application, simulations have been conducted over a range of Reynolds numbers ( $Re$ ) for a plain tube and a corrugated tube with and without twisted tapes. The enhancement in the heat transfer coefficient ( $Nu$ ) and rate of heat transfer ( $Q$ ) are compared. The Reynolds number range is from 33,000 to 68,000 for the gas in the inner tube.

#### 5.1. Simulations of the PTHE with Twisted Tapes

The simulation results show enhancements in heat transfer of about 35.5%, 27.0%, 21.1%, and 19.5% in the PTHEs with twisted tapes TT1, TT2, TT3, and TT4, respectively, when compared with the PTHE without twisted tape (Table 7). As expected, the tape with the maximum number of twists (TT1) provides more swirl and also yields the highest rate of heat transfer (8.5 kW).

The PTHE provides a heat transfer of 6.3 kW at a Reynolds number of 67,000. Table 7 and Figure 18 present and compare the rates of heat transfer for different twisted tape inserts in a PTHE. It can be observed that the Nusselt number increases with the number of twists. The maximum Nusselt number at the maximum Reynolds number in the PTHE with TT1 is 200.



Table 7: Heat transfer comparison for PTHE with TTs at a Reynolds number of 67,000

	PT	PT_TT1	PT_TT2	PT_TT3	PT_TT4
Heat transfer(W)	6328.6	8524.5	7989.7	7614.6	7516.5
Enhancement (%)	-	35.53	27.03	21.06	19.5

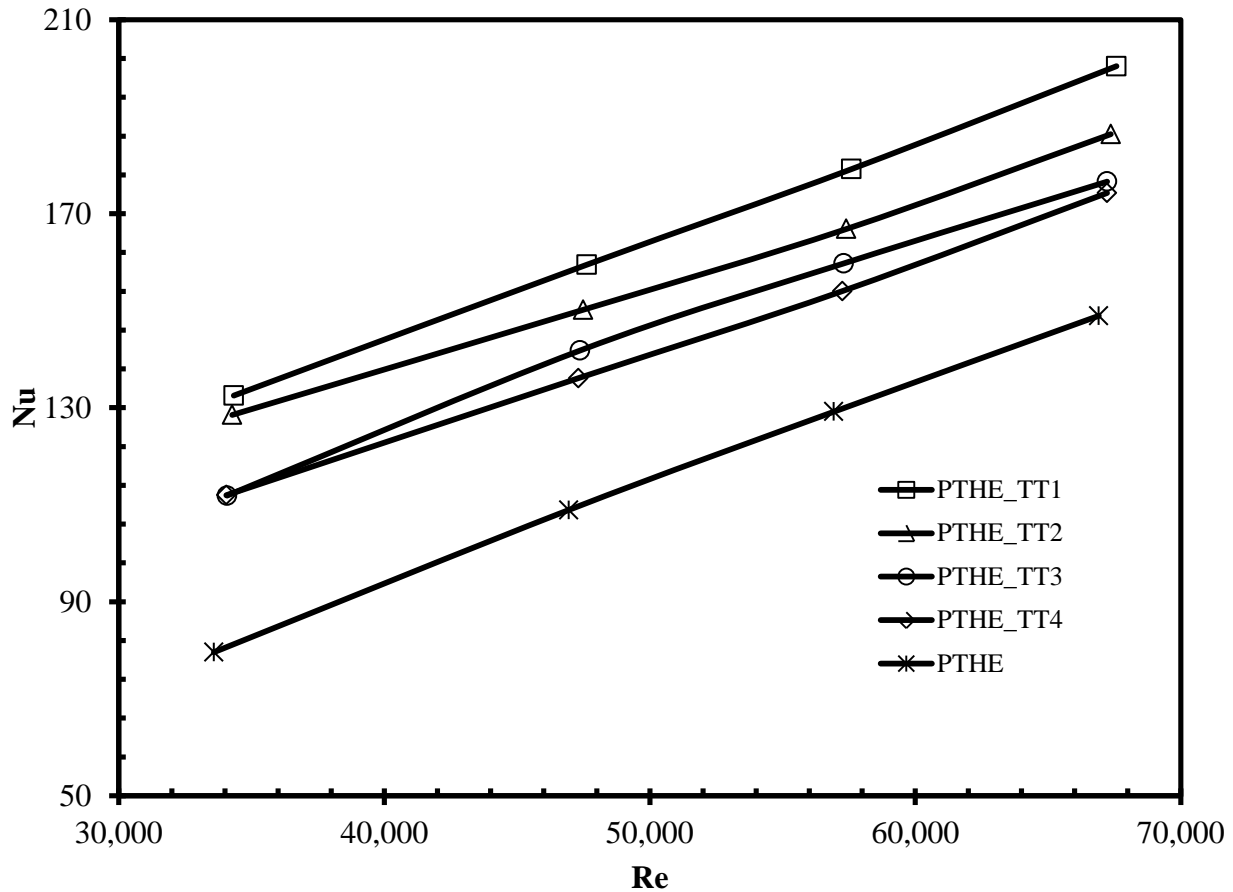


Figure 18: Nu versus Re for tubes with different twisted tape inserts.

## 5.2. Simulations of ACT Heat Exchangers with Twisted Tapes (TT1, TT2, TT3, and TT4)

The simulations for the ACTHE are conducted with similar boundary and inlet conditions to those used for the simulations with the PT. The total heat recovered by the ACT heat exchanger without twisted tape is around 11.48 kW. Simulations with twisted tapes are compared with the heat transfer of the PT and ACT heat exchangers. The heat transfer behavior in an annularly

corrugated tube with different twisted tapes at four different Reynolds numbers of gas is investigated and numerical simulation results for rate of heat transfer are presented in Tables 8 through 11, and comparison among them is presented in Figure 19.

Table 8: Simulation results of ACT heat exchanger with twisted tapes at Re = 77,700

	ACT	ACT_TT1	ACT_TT2	ACT_TT3	ACT_TT4
Heat transfer(W)	11487.3	19211.2	17217.42	15372.72	14162.57
$e$ (%) - PT <sup>a</sup>	81.5	203.7	172.1	142.9	123.8
$e$ (%) - ACT <sup>b</sup>	-	67.2	49.9	33.83	23.3

Table 9: Simulation results of ACT heat exchanger with twisted tapes at Re = 66,200

	ACT	ACT_TT1	ACT_TT2	ACT_TT3	ACT_TT4
Heat transfer(W)	10298.1	16828.29	15391.3	13952.96	12887.44
$e$ (%) - PT <sup>a</sup>	81.52	196.63	171.3	145.95	127.17
$e$ (%) - ACT <sup>b</sup>	-	63.41	50.98	38.59	27.13

Table 10: Simulation results of ACT heat exchanger with twisted tapes at Re = 53,000

	ACT	ACT_TT1	ACT_TT2	ACT_TT3	ACT_TT4
Heat transfer(W)	9040.96	14546.09	13650.8	12530.05	11494.28
$e$ (%) - PT <sup>a</sup>	88.6	203.44	184.77	161.38	139.78
$e$ (%) - ACT <sup>b</sup>	-	60.89	50.98	38.59	27.13

Table 11: Simulation results of ACT heat exchanger with twisted tapes at Re = 40,000

	ACT	ACT_TT1	ACT_TT2	ACT_TT3	ACT_TT4
Heat transfer(W)	7161.35	11765.7	10821.17	10379.16	9401.002
$e$ (%) - PT <sup>a</sup>	104.1	235.32	208.40	195.80	167.93
$e$ (%) - ACT <sup>b</sup>	-	64.294	51.105	44.93	31.27

<sup>a</sup>  $e$  (%) - PT refers the enhancement percentage when compared with PTHE without TTs;

<sup>b</sup>  $e$  (%) - ACT refers the enhancement percentage when compared with ACTHE without TTs.

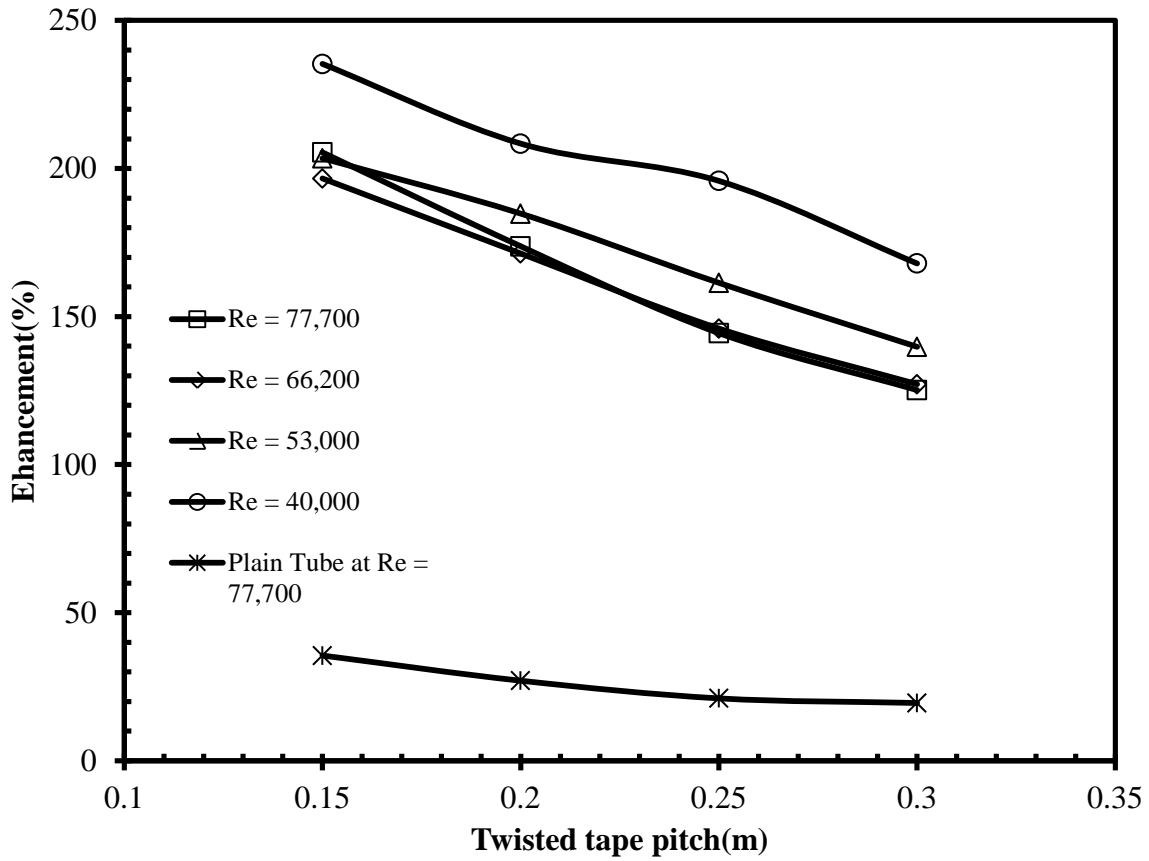


Figure 19: Twisted tape pitch versus enhancement percentage.

The heat transfer enhancement in an ACT HE with TT1 is about 235% and 64.2% at a Reynolds number of 40,000, and about 205.43% and 67.25% at a Reynolds number of 77,700, when compared with the PT and ACT heat exchangers without TTs, respectively.

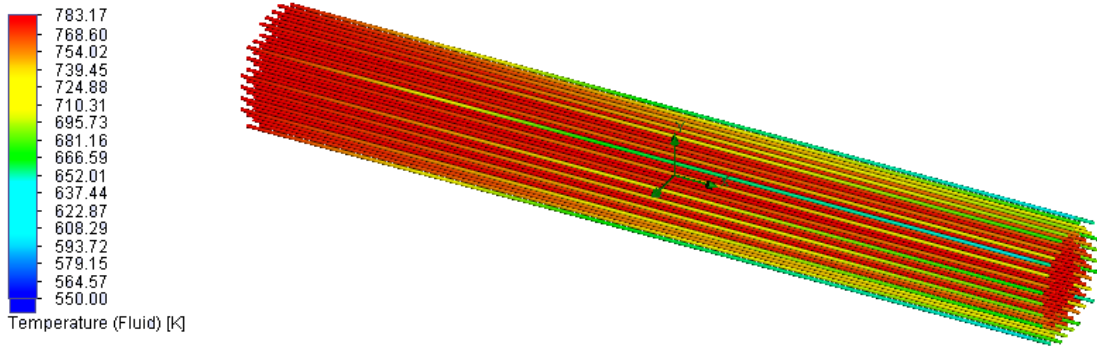


Figure 20: Flow trajectories with temperature distribution of gas inside a plain tube.

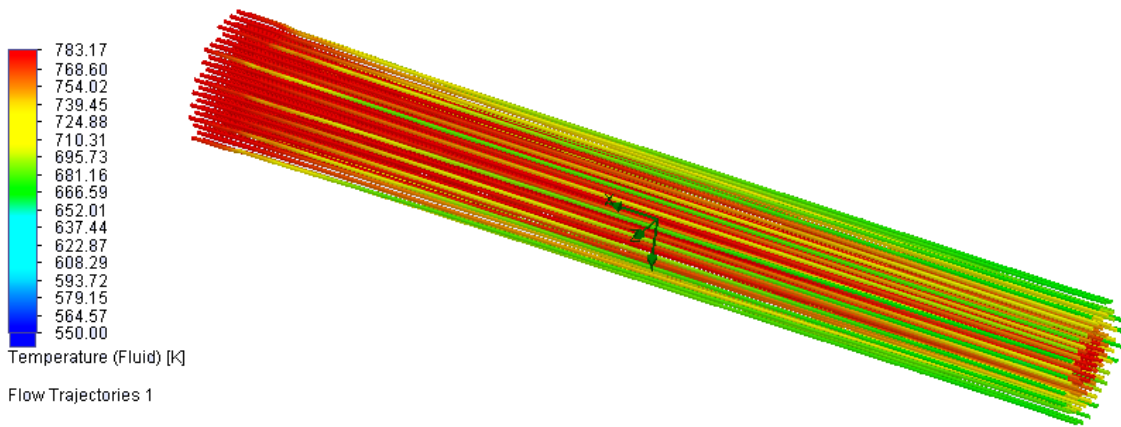


Figure 21: Flow trajectories with temperature distribution of gas inside an ACT.

The enhancement percentage of heat transfer rate in ACT heat exchangers with TTs is observed to be higher at low Reynolds numbers. The CFD program generated flow trajectories of gas inside PT and ACT HE without TT1 (Figs. 20, 21) and with TT1 (Figs. 22, 23), respectively. These figure also show the temperature variation of the gas from entrance to exit of the HE.

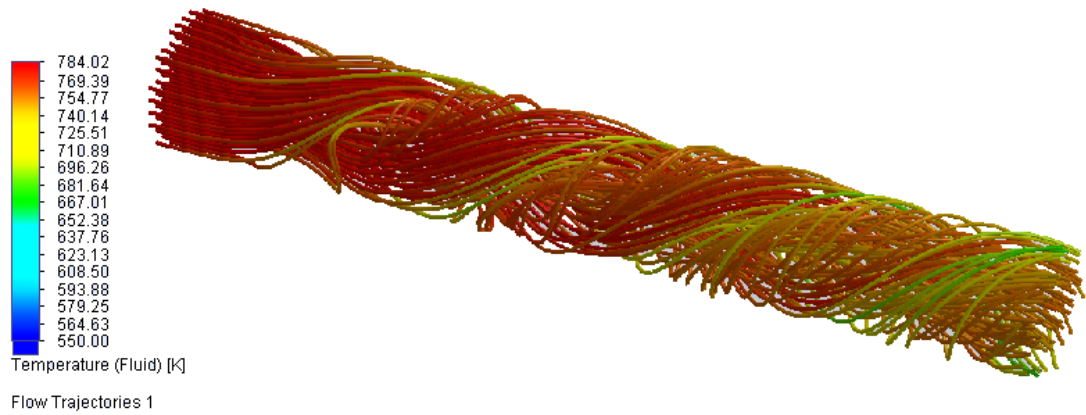


Figure 22: Flow trajectories and temperature distribution of gas inside a PT with TT1.

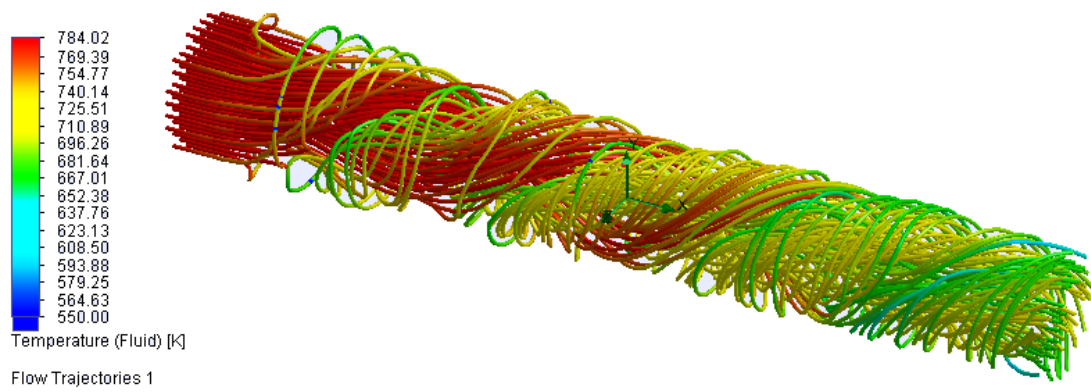


Figure 23: Flow trajectories and temperature distribution of gas inside an ACT with TT1.

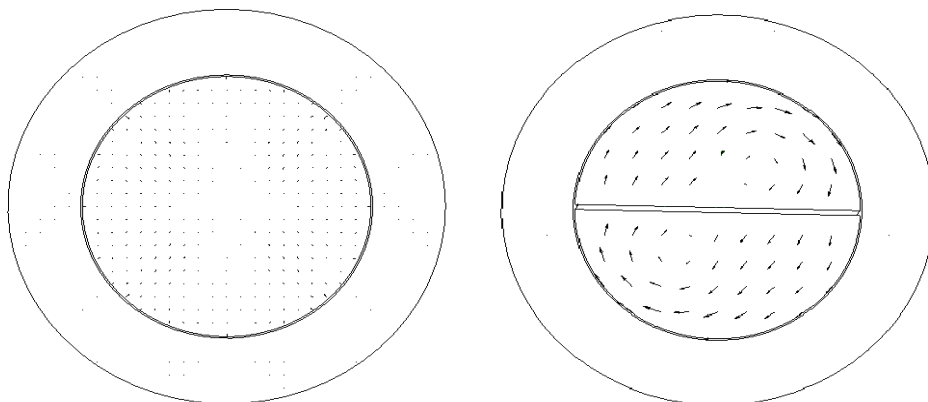


Figure 24: Velocity vectors inside an ACT and an ACT with TT1 at tube exit.

Figure 24 shows the direction of velocity vectors inside the ACT and ACT with TT1. The dots in this figure signify that there is no tangential velocity (i.e., only axial flow) inside the tube, and the arrows represent the direction of fluid flow.

Figure 25 compares the heat transfer rate of ACT and PTHEs with various twisted tape pitches ranging from 0.15 m to 0.3 m at a nitrogen volume flow rate of 0.3933 m<sup>3</sup>/s.

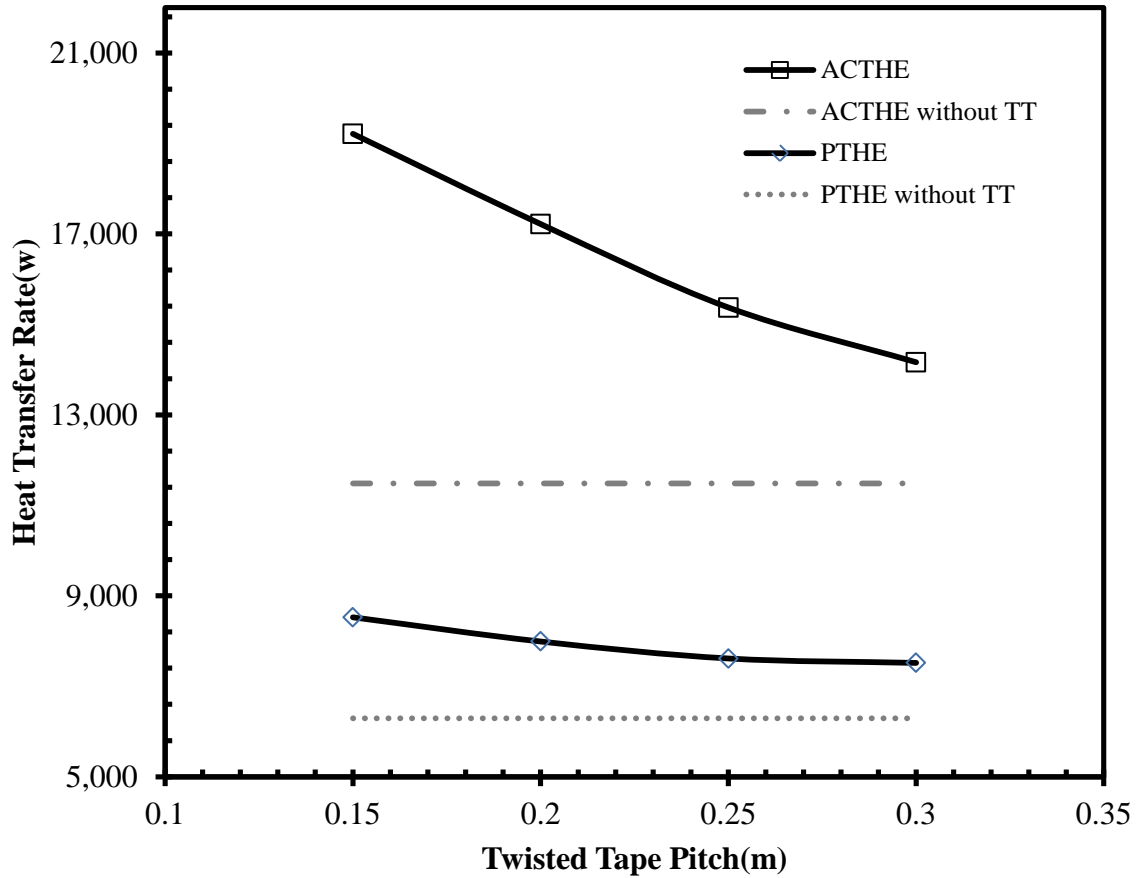


Figure 25: Heat transfer rate versus pitch of the twisted tape inserts in the ACTHE and PTHE.

Figure 26 presents the variation in the Nusselt number of ACT heat exchangers with different twisted tape inserts at different Reynolds numbers. The ACT with twisted tape (TT1) has the maximum Nusselt number of 201.75 at Reynolds number 77,700 when compared with

the other ACT heat exchangers with and without twisted tape inserts. TT1 has more twists and can generate more swirls in the ACT than other TTs, and hence its heat transfer coefficient is comparatively high.

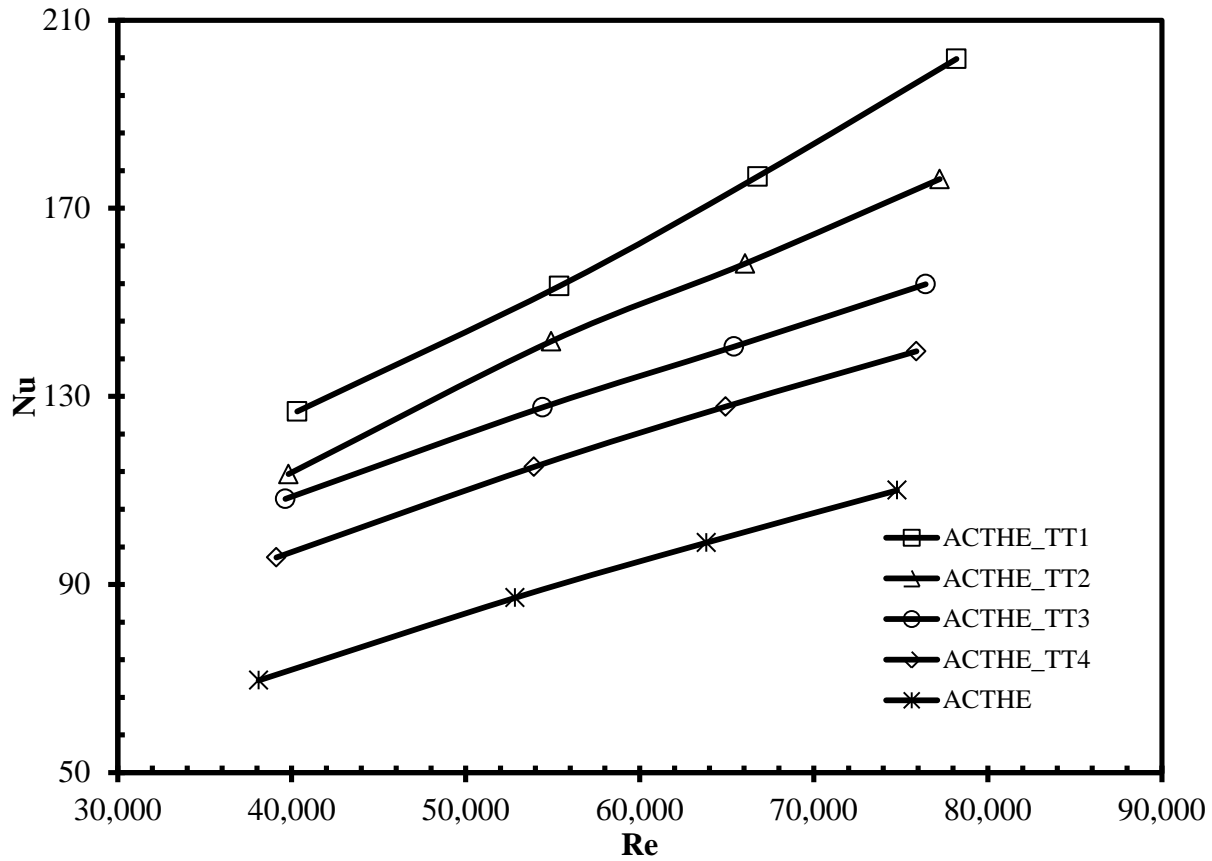


Figure 26: Nusselt number versus Reynolds number for ACT and ACT with TTs.

Figures 27 and 28 are contour plots of tangential velocity inside the plain tube and ACT without and with different twisted tapes, respectively. Higher tangential velocity, i.e., more swirling, is observed in the ACT under similar twisted tape and fluid flow conditions.

### 5.3. Effectiveness ( $\epsilon$ ) of PT and ACT Heat Exchangers

Using the equations mentioned in section 5.1, the effectiveness of the PT and ACT (with and without twisted tapes) heat exchangers under similar conditions are calculated from the simulation results.

The effectiveness of ACT HE with and without TT1 is about 23.67% and 14.35%, whereas the effectiveness of PTHE with and without TT1 is about 10.67% and 8.17% respectively. From Table 12, the effectiveness of PTHE is about 8.17%; when the PT is replaced by an ACT, effectiveness increases to 14.34%

Table 12: Heat exchanger effectiveness comparison

HE	Without TT	TT1	TT2	TT3	TT4
PT	8.17%	10.68%	10%	9.52%	9.4%
ACT	14.34%	23.6%	21.29%	19.05%	17.57%

#### 5.4. Economic Analysis

The economic analysis has been performed only on the heat recovery system which is readily available to install, i.e., an ACT heat exchanger with TT1. The Ruby village power plant diesel generator equipped with ACT vertical HE is able to recover 11.48 kW of heat from the diesel engine exhaust. The present ACTHE unit cost is \$2,215; the approximate cost of the twisted tape (TT1) is \$500 (estimated by a local machine shop). Simulation results show that using twisted tape with a pitch of 0.15m can enhance the heat recovery rate by up to 67.25%.

The cost of the twisted tape = \$500;

The total system cost = \$2,715 (i.e., unit cost + tape cost = \$2,215 + \$500)

Heating value for the fuel at 75% boiler efficiency = 101,250 BTU/gal

Total heat recovery rate of ACTHE= 11.48kW = 39,171.4 BTU/hr

$$\text{Heat recovered per year} = 39,171.36 \frac{\text{BTU}}{\text{hr}} \times 24 \frac{\text{hrs}}{\text{day}} \times 363 \frac{\text{days}}{\text{yr}} = 341.4 \text{ MBTU/yr}$$

Based on a fuel cost of \$5.00 per gallon, which is common for rural Alaskan villages, the estimated payback period for an ACT heat exchanger with TT1 is about 1 month, with little to no increased maintenance. A summary of the economic analysis is listed in the first row of Table 13.



Saving fuel not only saves money but also reduces the amount of CO<sub>2</sub> released into the atmosphere. About 10.15 kg of CO<sub>2</sub> is released by burning one gallon of heating oil [36]. Using an ACTHE with twisted tape can save up to 5,636.5 gallons of fuel per year while also reducing emissions of CO<sub>2</sub> by up to 23 metric tons a year.

Table 13: Economic analysis

Heat Exchanger	ACT (Current Installation)	ACT with TT1(Proposed Installation)
Initial Unit Cost	\$2,150	\$2,650
Heat Recovered Annually	341.22 MBtu/year	570.69 MBtu/year
Annual Fuel Savings	3,370.1 gals/year	5,636.5 gals/year
Annual Savings	\$16,850/year	\$28,181/year
Estimated Payback Period	1.5 months	1 month
CO <sub>2</sub> Savings	34.2 metric tons	57.2 metric tons

### 5.5. Discussion of Results

Simulation results show that, for the same heat exchanger dimensions (i.e., height and diameter), the heat transfer rate of an ACTHE (11.4 kW) is higher than that of a PTHE (6.3 kW). This may result from the greater surface area of the ACTHE.

The results also show that the twisted tape (TT) inserts can improve heat transfer related performance parameters, such as the Nusselt number (Fig. 17), heat transfer enhancement (Fig. 18), and heat transfer rates (Tables 8 to 11) against both plain and corrugated tubes. This is due to the swirl generated by the twist tape inserts (Figures 19 to 22).

Figures 19 and 21 show that the flow swirl (represented by stream lines) of a plain tube with a TT1 insert is much higher than that of a plain tube without a TT. A similar observation is shown in Figures 20 and 22 for a corrugated tube.

According to Figures 18 and 19, the flow trajectories inside a plain tube and an annularly corrugated tube are very similar to each other; the advantages of corrugations are not completely

utilized. Inserting the twisted tape in the plain tube and corrugated tubes increases the swirling of the fluid and decreases temperature more in the corrugated tube than in the plain tube (Figs. 21 and 22).

From Tables 8 through 11, it can be found that, for similar Reynolds numbers, greater enhancement percentages resulted from TT insertion into corrugated tubes (Table 9). Enhancements in corrugated tubes, between 23.3% and 67.26%, are significantly higher than for plain tubes (enhancement between 19.5% and 35.53%), (Table 8). The cause may be that the corrugated tube helps promote swirl, increasing heat transfer.

From observation, the heat transfer rate increases as the pitch of the TT decreases (Fig. 25). This may be because a shorter pitch means more the twists for the same length HE. More twists may guide the fluid to travel and turn more, causing higher tangential velocity inside the HE (Figs. 27 and 28). However, too many turns of the twisted tape may increase the pressure drop considerably.

From Figure 18, enhancement percentages are 235.32% and 205.43% at Reynolds numbers of 40000 and 77000, respectively. The twisted tapes are performing more effectively at lower flow rates in an annularly corrugated tube. From Table 12, the effectiveness of PTHE is about 8.17%; when the PT is replaced by an ACT, effectiveness increases to 14.34%. However, inserting twisted tape in the ACTHE increases effectiveness to 23.6%, which is about 9.26% more than that of the PTHE. According to the simulation results, a maximum enhancement in rate of heat transfer of ~67.25% is observed when TT1 is inserted in the current heat recovery system of the Ruby power plant.

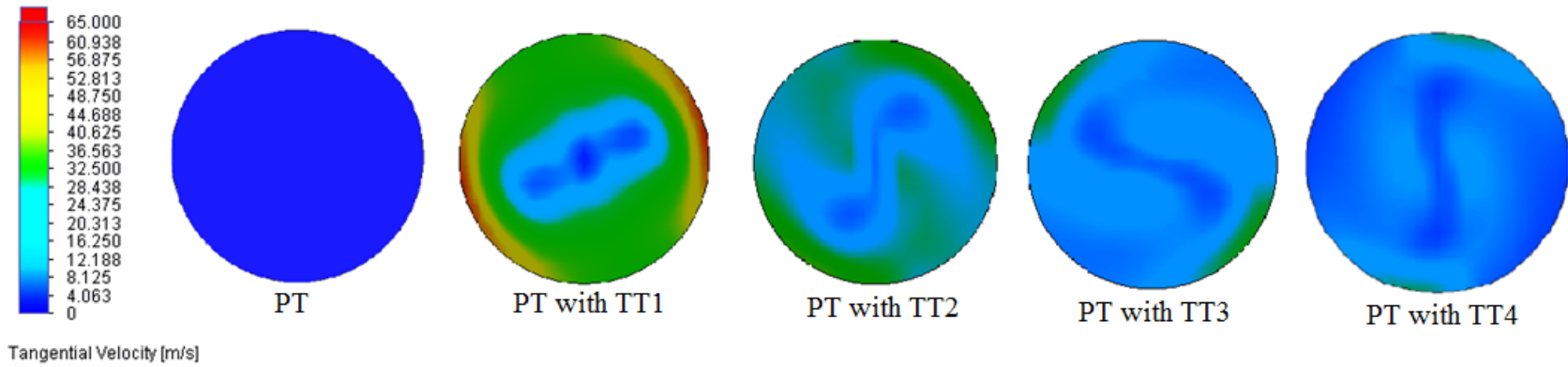


Figure 27: Tangential velocity contour plot at exit of PTHE without and with TT (1-4)

44

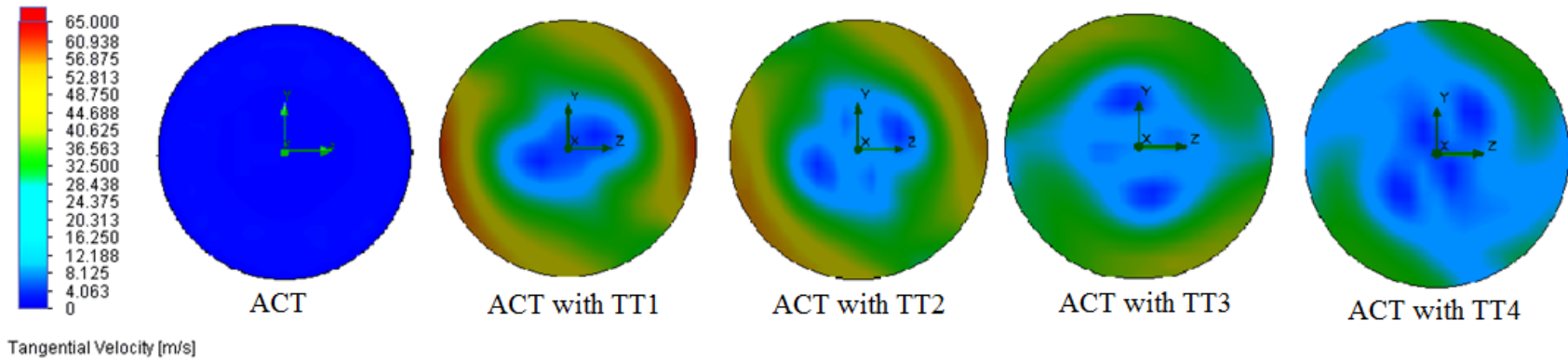


Figure 28: Tangential velocity contour plot at the exit of an ACTHE without and with TT (1-4)

## Chapter 6. Annularly Corrugated Tube Heat Exchanger with Modified Twisted Tape Inserts

This chapter discusses the optimization of twisted tape inserts with minor modifications. From the observation of simulation results for annularly corrugated tubes with twisted tape inserts, the twisted tape with a highest twist ratio (pitch) enhanced the heat recovery the most.

Twisted tape inserts with a twist ratio of 0.15 m, used in the previous section, are modified in order to investigate the further enhancement of the exhaust heat recovery at various flow rates of exhaust gas. The modified twisted tapes are perforated, serrated, and provided with hollow rods—all modifications adopted from the literature search for liquid to liquid heat exchangers. Figure 29 presents a 3D model of the modified twisted tapes.

### 6.1. Simulations of ACT Heat Exchanger with Modified Twisted Tapes

Modified twisted tapes are inserted into an ACTHE and then simulated under similar boundary and initial conditions to those mentioned in Chapter 3. The results obtained are processed using equations mentioned in section 5.1.

The simulation results for an ACTHE with modified twisted tapes are presented in Figure 30 as a graph of Nussult number versus Reynolds number. The figure clearly shows that the twisted tape with rod has the highest heat transfer coefficient.

Out of the various modified twisted tapes mentioned in Figure 29, the twisted tape with rod has improved the rate of heat recovery significantly, while all the other twisted tapes have a heat recovery rate identical to that of the classical twisted tape. This can be observed in Figure 30.



A) Perforated Twisted Tape



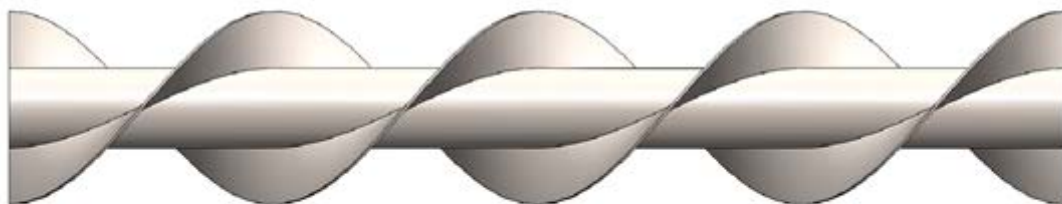
B) Dual Twisted Tape



C) Twisted Tape with Cut



D) Serrated Twisted Tape



E) Twisted Tape with Rod

Figure 29: Modified twisted tape inserts.

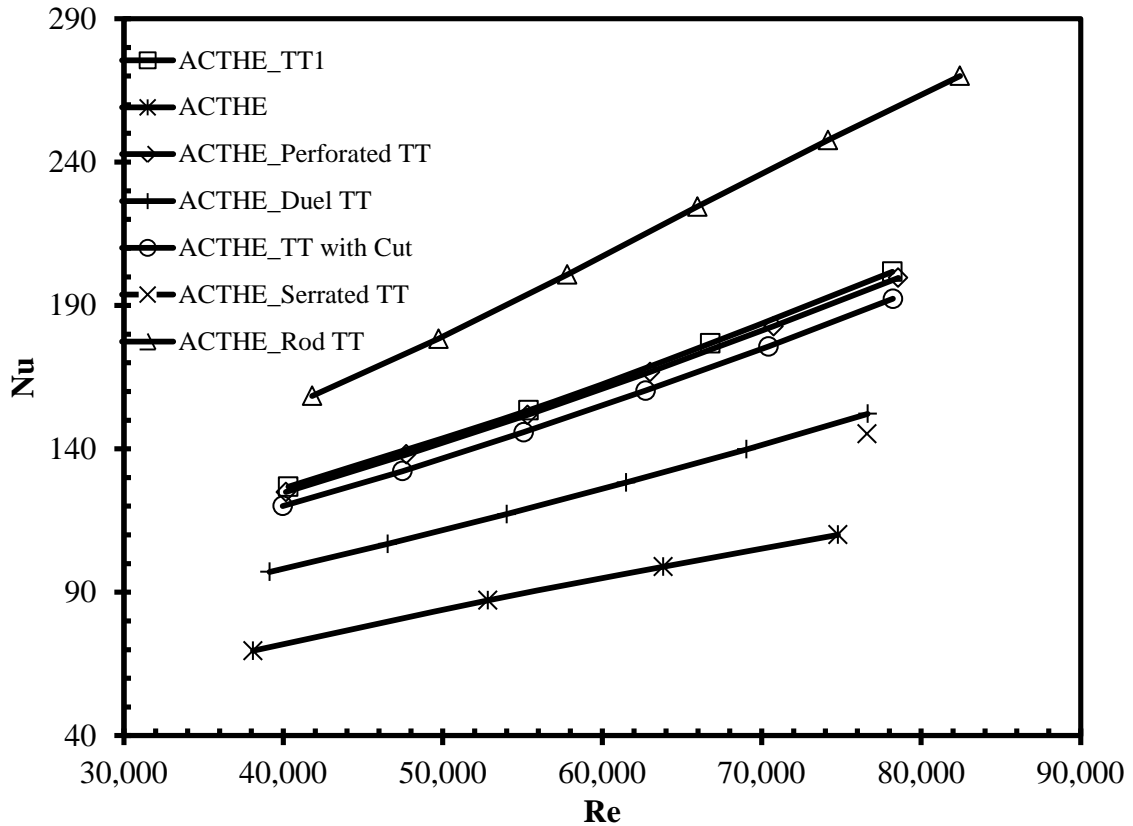
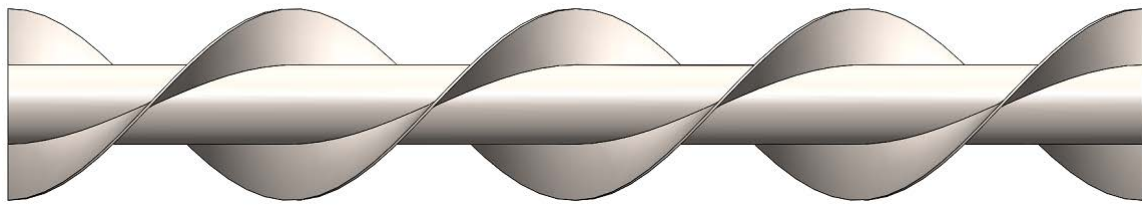


Figure 30: Nusselt number versus Reynolds number for ACT and ACT with modified TTs.

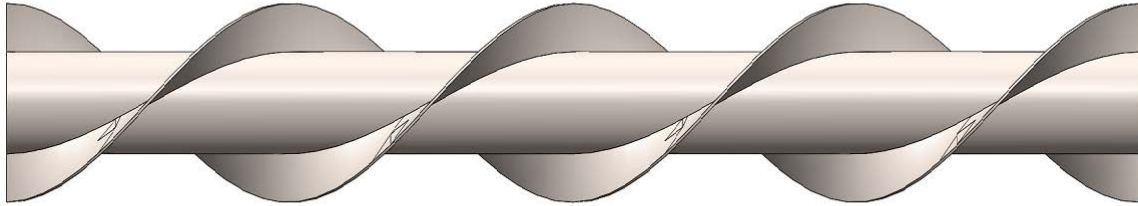
## 6.2. Simulations of ACT Heat Exchanger with Rod Twisted Tape (RTT)

The use of twisted tape with rod (RTT) gives a higher heat transfer due to a greater contact surface area. To optimize the suitable twisted tape for exhaust heat recovery application, simulations are performed with different twisted tapes with similar pitch but varying center rod diameter. Figure 31 shows a 3D model of twisted tapes with rods of various diameters.

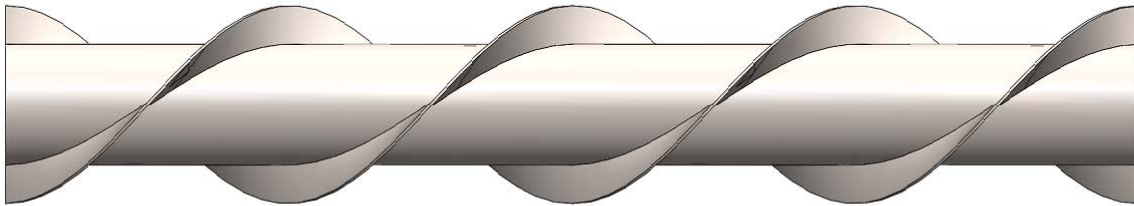
This type of twisted tape with rod reduces the flow area and increases the rotational velocity of the fluid. The larger the center rod diameter, the higher the rotational velocity of the fluid and the smaller the flow area. This can greatly impact the pressure drop. Since the pressure drop is one major criterion for exhaust heat recovery, pressure drop analysis is also performed to ensure the pressure drop is within an acceptable range.



A) Rod Diameter = 0.04m



B) Rod Diameter = 0.05m



C) Rod Diameter = 0.06m

Figure 31: Modified twisted tape inserts with rods: A) RTT1; B) RTT2; C) RTT3.

The twisted tape with rod diameter 0.04 m (RTT1) has the maximum heat transfer performance of about 24kW at a pressure drop of about 4.79kPa, which is well under the acceptable range of 6.7 to 10.2 kPa [30].

Figure 32, below, presents the heat recovery rate versus pressure drop. The optimum point is where the heat recovery rate is highest and the pressure drop is lowest.

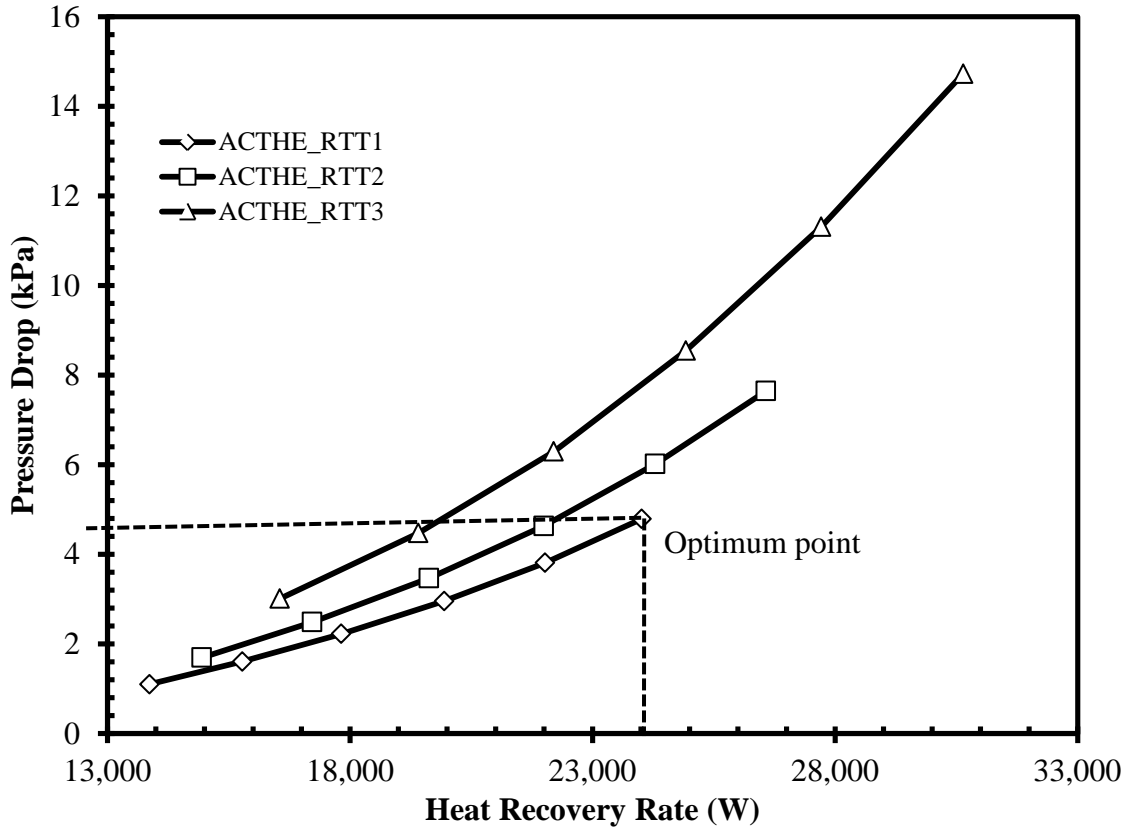


Figure 32: Heat recovery rate versus pressure drop of ACTHE with rod TTs.

Table 14 presents heat exchanger effectiveness comparison between PTHE, ACTHE with TT1, RTT1, RTT2 and RTT3. Figure 33 gives a Reynolds number versus Nusselt number plot for an ACT heat exchanger with both classical twisted tape and twisted tape with rod (optimal RTT).

Table 14: Heat exchanger effectiveness

HE	Without TT	TT1	RTT1	RTT2	RTT3
ACT	14.34%	23.6%	30.25%	37.67%	48.89%



### 6.3. Effectiveness ( $\epsilon$ ) of ACT Heat Exchangers with TT1 and Rod TT ( $D= 0.04\text{ m}$ )

Using the equations mentioned in section 5.1, the effectiveness of the ACT heat exchanger with RTT and TT1 are calculated under similar conditions. The effectiveness of ACTHE with TT1 is about 23.67% and the effectiveness of ACTHE with RTT1 is about 30.25%, which is about 27% more.

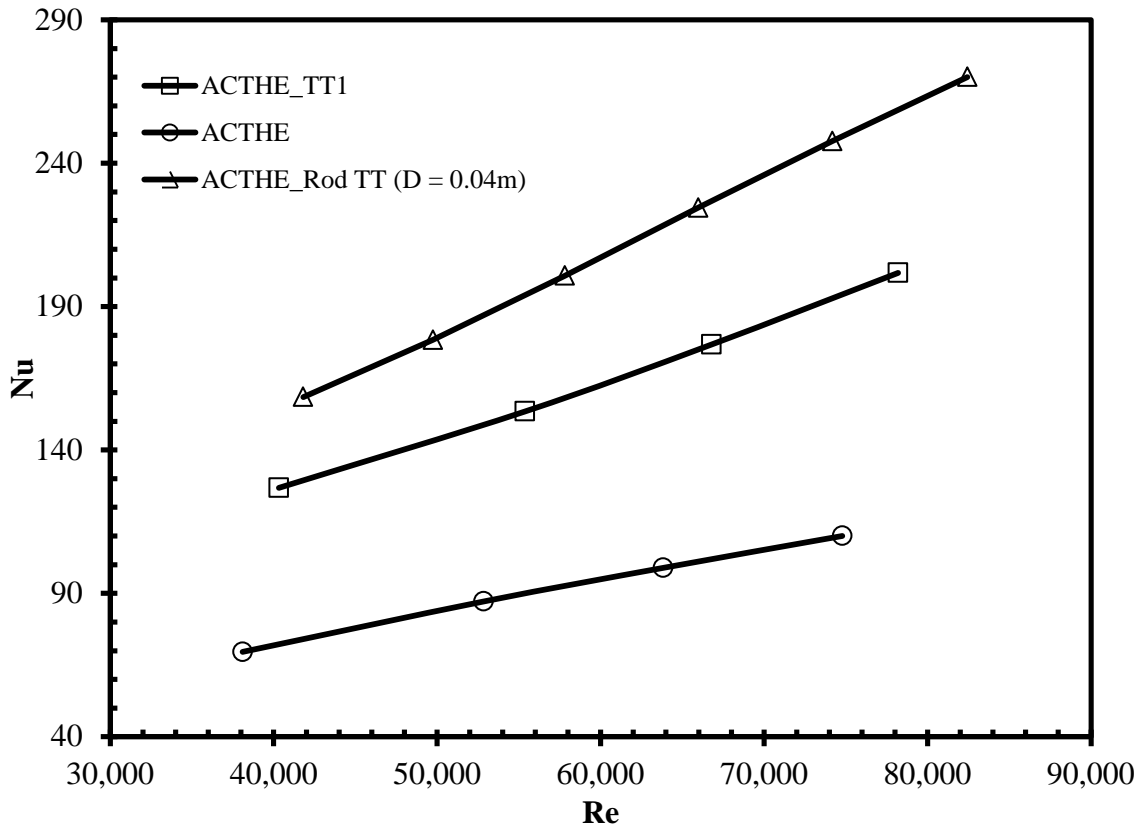


Figure 33: Reynolds number versus Nusselt number for ACTHE with TT1 and RTT1.

Though other rod twisted tapes (e.g., RTT2, RTT3) can promote the effectiveness of the heat exchanger significantly, they are not suitable for this application due to higher pressure drops.

#### 6.4. Discussion of Results

The economic analysis is not performed for a heat recovery unit with RTT1 insertion, as the cost for this type of twisted tape is unknown. The RRT1 is optimized to maximize heat recovery. Simulation results show that twisted tape with a rod of diameter 0.04 m (RTT1) can provide the maximum heat recovery of about 24 kW with an acceptable pressure drop of about 4.79 kPa, whereas the classical twisted tape (TT1) can recover about 19.2 kW with a pressure drop of 2.2 kPa.

RTT1 increases ACT heat exchanger effectiveness from 14.34% to 30.25%, which is quite significant. ACT heat exchangers with RTT1 can enhance recover about 27% and 110% more heat than ACTHE with TT1 and ACTHE, respectively. Although the effectiveness of ACTHE with RTT2 and RTT3 is more than that of RTT1, the pressure drop is close to the unacceptable range. As a matter of safety, RTT1 is the most effective twisted tape to maximize the heat recovery.



## Chapter 7. Conclusions

A study to improve the effectiveness of a diesel exhaust heat recovery system (concentric tube heat exchanger with annularly corrugated tube) in Ruby, Alaska has been conducted. The improved system is the original heat exchanger with a twisted tape insert. The goal of the present work is to maximize the heat recovery rate through minor modifications to the current heat recovery system. The physical size of the heat exchanger, twist ratio, and exhaust back pressure change are the constraints of the system. This study uses a plain outer tube and tests different inner tube configurations like a helically corrugated tube and an annularly corrugated tube with and without a twisted tape inserts. The following paragraphs summarize the findings obtained from this study.

A twisted tape insert was found to cause significant improvement in heat transfer performance of the plain tube heat exchanger. Among all the twisted tapes tested (TT1, TT2, TT3, and TT4) the one with lowest pitch (i.e. TT1, ~0.15 m) has the greatest effect on the heat transfer enhancement, which is about 35.5%.

The corrugated tube heat exchanger improves the rate of heat transfer up to 82% and 35% when compared with the plain tube without and with TT1, respectively. The annularly corrugated tube heat exchanger with a twisted tape insert has more heat transfer than one without twisted tape. The twisted tape insert caused significant improvement in the heat transfer performance of corrugated tube heat exchangers as well. Inserting the twisted tapes TT1, TT2, TT3, and TT4 in the ACT heat exchanger increased the heat transfer rates by 67.25%, 49.89%, 33.83%, and 23.3 %, respectively, when compared with the ACTHE without twisted tape.

The heat transfer rate in a corrugated tube heat exchanger with twisted tape inserts is 67% more than that of a corrugated tube alone. When the same twisted tape is inserted in the plain tube heat exchanger, the heat transfer rate is about 35.3% more than that of a plain tube alone. This clearly states that the corrugated tube is promoting more swirl than the plain tube.

Among all the twisted tapes tested (TT1, TT2, TT3, and TT4), the one with lowest pitch, i.e., TT1 (~0.15m), has the greatest effect on heat transfer enhancement and heat exchanger effectiveness. This particular twisted tape with 0.15 m pitch is modified slightly with holes, serrated surfaces, a rod, etc., to investigate changes in heat transfer performance. A twisted tape with rod (RTT1) has improved the heat transfer rate by about 25% compared to the classical twisted tape (TT1), while the other modified twisted tapes performed similarly to or were less effective than TT1.

RTT1 shows some improvement in the rate of heat transfer but the pressure drop is also drastically increased when this type of twisted tape is used. Simulations are performed to optimize the twisted tape with rod and RTT1 has the maximum heat recovery rate (i.e. 24 kW) along with the pressure drop of 4.79 kPa, which is below a cut-off point.

Since the annular corrugated tube heat exchanger with classical twisted tape insert combination is readily available, the economic analysis is performed only on this heat recovery system. Using an ACTHE with twisted tape can save up to 5,636.5 gallons of fuel per year (2,266 gallons more than the presently installed heat recovery system) and also reduce emissions of CO<sub>2</sub> by up to 23 metric tons annually. The payback period for the proposed exhaust heat recovery system is about 1 month, in comparison with that of the currently installed setup, which is 1.5 months.

The pressure drop of the exhaust gas in the selected heat recovery system (ACTHE with TT1) is about 0.257 psi (1.77 kPa), which conveys that the effect of inserting twisted tape on the engine performance is minimal. Based on this study, the proposed exhaust heat recovery system with TT1 is easy to install, relatively inexpensive, easy to maintain, and has no practical effect on exhaust emissions. It would also have a good economic effect on the Ruby diesel power plant. If the system were applied to all the diesel generators in rural Alaskan villages, the potential savings could be \$4 million per year, based on 370,000 MW-h power consumption in 2011 [37].

## References

- [1] J. G. Withers, "Tube-Side Heat Transfer and Pressure Drop for Tubes Having Helical Internal Ridging with Turbulent/Transitional Flow of Single-Phase Fluid. Part 1. Single-Helix Ridging," *Heat Transfer Engineering*, vol. 2, p. 10, 1980.
- [2] L. Wang, D.-W. Sun, P. Liang, L. Zhuang, and Y. Tan, "Heat transfer characteristics of carbon steel spirally fluted tube for high pressure preheaters," *Energy Conversion and Management*, vol. 41, pp. 993-1005, 7/1/ 2000.
- [3] P. G. Vicente, A. García, and A. Viedma, "Mixed Convection Heat Transfer and Isothermal Pressure Drop in Corrugated Tubes for Laminar and Transition Flow," *International Communications in Heat and Mass Transfer*, vol. 31, pp. 651-662, 2004.
- [4] S. Pethkool, S. Eiamsa-ard, S. Kwankaomeng, and P. Promvongse, "Turbulent heat transfer enhancement in a heat exchanger using helically corrugated tube," *International Communications in Heat and Mass Transfer*, vol. 38, pp. 340-347, 2011.
- [5] Ö. Agra, H. Demir, Ş. Ö. Atayılmaz, F. Kantaş, and A. S. Dalkılıç, "Numerical investigation of heat transfer and pressure drop in enhanced tubes," *International Communications in Heat and Mass Transfer*, vol. 38, pp. 1384-1391, 2011.
- [6] A. García, J. P. Solano, P. G. Vicente, and A. Viedma, "The influence of artificial roughness shape on heat transfer enhancement: Corrugated tubes, dimpled tubes and wire coils," *Applied Thermal Engineering*, vol. 35, pp. 196-201, 2012.
- [7] H.-Z. Han, B.-X. Li, B.-Y. Yu, Y.-R. He, and F.-C. Li, "Numerical study of flow and heat transfer characteristics in outward convex corrugated tubes," *International Journal of Heat and Mass Transfer*, vol. 55, pp. 7782-7802, 2012.
- [8] P. Poredoš, T. Šuklje, S. Medved, and C. Arkar, "An experimental heat-transfer study for a heat-recovery unit made of corrugated tubes," *Applied Thermal Engineering*, vol. 53, pp. 49-56, 2013.
- [9] H. A. Mohammed, A. K. Abbas, and J. M. Sheriff, "Influence of geometrical parameters and forced convective heat transfer in transversely corrugated circular tubes," *International Communications in Heat and Mass Transfer*, vol. 44, pp. 116-126, 2013.

- [10] S. Al-Fahed, L. M. Chamra, and W. Chakroun, "Pressure drop and heat transfer comparison for both microfin tube and twisted-tape inserts in laminar flow," *Experimental Thermal and Fluid Science*, vol. 18, pp. 323-333, 1999.
- [11] S. K. Saha, A. Dutta, and S. K. Dhal, "Friction and heat transfer characteristics of laminar swirl flow through a circular tube fitted with regularly spaced twisted-tape elements," *International Journal of Heat and Mass Transfer*, vol. 44, pp. 4211-4223, 11// 2001.
- [12] S. Ray and A. W. Date, "Friction and heat transfer characteristics of flow through square duct with twisted tape insert," *International Journal of Heat and Mass Transfer*, vol. 46, pp. 889-902, 2// 2003.
- [13] A. García, P. G. Vicente, and A. Viedma, "Experimental study of heat transfer enhancement with wire coil inserts in laminar-transition-turbulent regimes at different Prandtl numbers," *International Journal of Heat and Mass Transfer*, vol. 48, pp. 4640-4651, 2005.
- [14] S. Eiamsa-ard and P. Promvonge, "Enhancement of heat transfer in a tube with regularly-spaced helical tape swirl generators," *Solar Energy*, vol. 78, pp. 483-494, 2005.
- [15] S. Eiamsa-ard, C. Thianpong, and P. Promvonge, "Experimental investigation of heat transfer and flow friction in a circular tube fitted with regularly spaced twisted tape elements," *International Communications in Heat and Mass Transfer*, vol. 33, pp. 1225-1233, 2006.
- [16] P. Naphon and P. Sriromrui, "Single-phase heat transfer and pressure drop in the micro-fin tubes with coiled wire insert," *International Communications in Heat and Mass Transfer*, vol. 33, pp. 176-183, 2006.
- [17] S. W. Chang, T. L. Yang, and J. S. Liou, "Heat transfer and pressure drop in tube with broken twisted tape insert," *Experimental Thermal and Fluid Science*, vol. 32, pp. 489-501, 2007.
- [18] P. Promvonge and S. Eiamsa-ard, "Heat transfer behaviors in a tube with combined conical-ring and twisted-tape insert," *International Communications in Heat and Mass Transfer*, vol. 34, pp. 849-859, 2007.
- [19] P. Promvonge, "Thermal performance in circular tube fitted with coiled square wires," *Energy Conversion and Management*, vol. 49, pp. 980-987, 2008.

- [20] P. Promvonge, "Thermal augmentation in circular tube with twisted tape and wire coil turbulators," *Energy Conversion and Management*, vol. 49, pp. 2949-2955, 2008.
- [21] P. Bharadwaj, A. D. Khondge, and A. W. Date, "Heat transfer and pressure drop in a spirally grooved tube with twisted tape insert," *International Journal of Heat and Mass Transfer*, vol. 52, pp. 1938-1944, 2009.
- [22] M. Rahimi, S. R. Shabaniyan, and A. A. Alsairafi, "Experimental and CFD studies on heat transfer and friction factor characteristics of a tube equipped with modified twisted tape inserts," *Chemical Engineering and Processing: Process Intensification*, vol. 48, pp. 762-770, 2009.
- [23] S. Eiamsa-ard, K. Wongcharee, and S. Sripattanapipat, "3-D Numerical simulation of swirling flow and convective heat transfer in a circular tube induced by means of loose-fit twisted tapes," *International Communications in Heat and Mass Transfer*, vol. 36, pp. 947-955, 2009.
- [24] C. Thianpong, P. Eiamsa-ard, K. Wongcharee, and S. Eiamsa-ard, "Compound heat transfer enhancement of a dimpled tube with a twisted tape swirl generator," *International Communications in Heat and Mass Transfer*, vol. 36, pp. 698-704, 2009.
- [25] S. W. Chang and M. H. Guo, "Thermal performances of enhanced smooth and spiky twisted tapes for laminar and turbulent tubular flows," *International Journal of Heat and Mass Transfer*, vol. 55, pp. 7651-7667, 2012.
- [26] S. Eiamsa-ard and P. Seemawute, "Decaying swirl flow in round tubes with short-length twisted tapes," *International Communications in Heat and Mass Transfer*, vol. 39, pp. 649-656, 2012.
- [27] T. Chompookham, C. Thianpong, S. Kwankaomeng, and P. Promvonge, "Heat transfer augmentation in a wedge-ribbed channel using winglet vortex generators," *International Communications in Heat and Mass Transfer*, vol. 37, pp. 163-169, 2010.
- [28] M. M. K. Bhuiya, M. S. U. Chowdhury, M. Saha, and M. T. Islam, "Heat transfer and friction factor characteristics in turbulent flow through a tube fitted with perforated twisted tape inserts," *International Communications in Heat and Mass Transfer*, vol. 46, pp. 49-57, 2013.



- [29] S. Eiamsa-ard, P. Somkleang, C. Nuntadusit, and C. Thianpong, "Heat transfer enhancement in tube by inserting uniform/non-uniform twisted-tapes with alternate axes: Effect of rotated-axis length," *Applied Thermal Engineering*, vol. 54, pp. 289-309, 2013.
- [30] A. Mayer. (2004). Number-based Emission Limits, VERT-DPF-Verification Procedure and Experience with 8,000 Retrofits.
- [31] "SolidWorks Flow Simulation 2012" ,Technical Reference, 2012.
- [32] D. P. D. Frank P. Incropera, "Introduction to Heat Transfer", John Wiley & Sons, 1996.
- [33] V. E. G. Biswas, "Turbulent Flows : Fundamentals, Experimental and Modeling," CRC Press, p. 456, 2002.
- [34] "Ruby Power Plant Exhaust Heat Recovery Testing.", Alaska Energy and Engineering, Inc., 2011
- [35] D. P. S. Ramesh K. Shah, *Fundamentals of Heat Exchanger Design*, 2003.
- [36] U.S. Energy Information Administration, [www.eia.gov/oiaf/1605/coefficients.html](http://www.eia.gov/oiaf/1605/coefficients.html), 2011.
- [37] C.S.Lin., "Capture of Heat Energy from Diesel Engine Exhaust," Final report prepared for National Energy Technology Laboratory, DOE Award #DE-FC26-01NT41248, November 2008.